Porous Barium-Organic Frameworks with Highly Efficient Catalytic Capacity and Fluorescent Sensing Ability

Fuling Liu,[b] Yuwen Xu,[a] Lianming Zhao,[a] Liangliang Zhang,[a] Wenyue Guo,[a*] Rongming Wang,[a] and Daofeng Sun*[a]

[a] State Key Laboratory of Heavy Oil Processing, China University of Petroleum (East China), College of Science, China University of Petroleum (East China), Qingdao, Shandong, 266580, China.

[b] Key Lab of Colloid and Interface Chemistry, Ministry of Education, School of Chemistry and Chemical Engineering, Shandong University, No. 27, Shanda South Road, Jinan City, Shandong Province, P.R. China

Content

(1) Experimental Procedures

Unless otherwise noted, all reagents were obtained from commercial suppliers and used without further purification. ^{1}H NMR spectra was measured on a Bruker AVANCE-300 NMR Spectrometer. X-ray powder diffractions were measured on a Panalytical X-Pert pro diffractometer with Cu-Kα radiation. Elemental analyses (C, H, N) were obtained on a PerkinElmer 240 elemental analyzer. The thermogravimetric analysis (TGA) for complexes **1** and **2** was carried out between room temperature and 600 °C in a static N_2 with a heating rate of 10°C/min. Photoluminescence spectra were measured on F-280 fluorescence spectrophotometer. ^{1}H NMR spectra were recorded on a 300 MHz spectrometer. Low pressure (< 800 torr) gas (N_2, CO_2 and CH_4) sorption isotherms were measured using a Micrometrics ASAP 2020 surface area and pore size analyzer. Prior to the measurements, the samples were degassed for 10 h at 120 °C. Ultra-high purity (UHP grade 5.0, 99.999% purity) gases were used for all measurements. Oil-free vacuum pumps and oil-free pressure regulators were used for all measurements to prevent contamination of the samples during the degassing process and isotherm measurement. Approximately 120 mg of activated sample was used for all measurements.

(2) Synthesis of H_4L^{OMe}

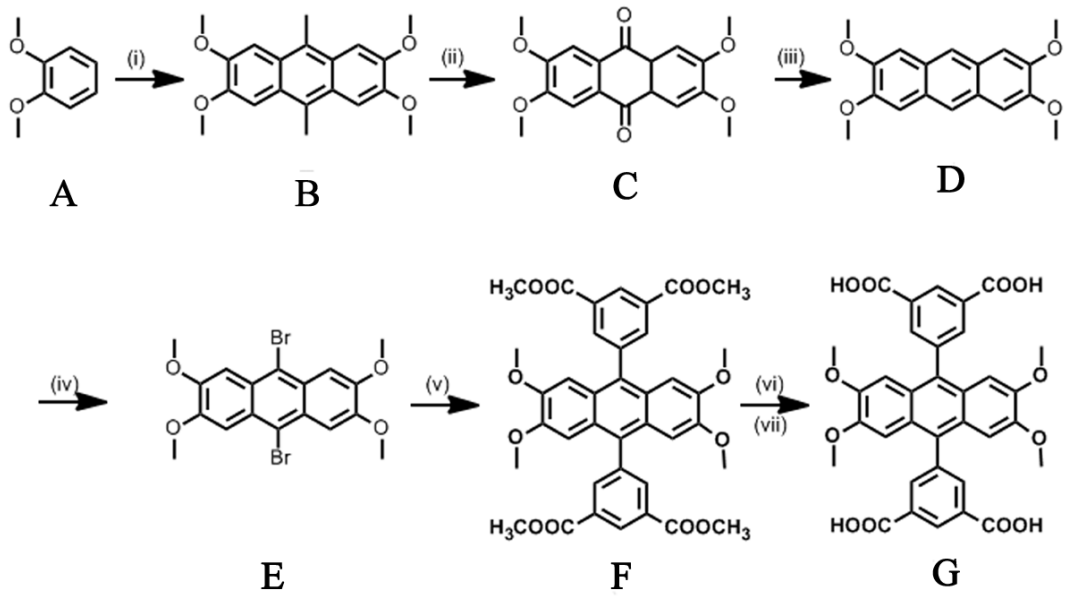

Synthesis of B: To a cooled solution (0 ^oC) of veratrole (**A**) (32 mL, 250 mmol) in acetic acid (125 mL) was slowly added ice-cold solution of acetaldehyde (21 mL,375 mmol) in methanol (20 mL). The resulting mixture was then stirred for 1h and concentrated H_2SO_4 (95 %, 125 mL) was added dropwise over 2h. The reaction mixture was then stirred at 0 ^oC for 20 hours, and poured into ice-water which precipitated the product out as beige solid and collected by vacuum filtration. The product washed with water and dried. It was further-purified by column chromatography (silica, $CHCl_3$) to afford the final product as a yellow solid (47.4 % yield). ^1H NMR ($CDCl_3$): δ = 7.40 (s, 4H), 4.08 (s, 12H), 2.95 (s, 6H).

Synthesis of C: A mixture of finely powdered **B** (10.0 g, mmol), sodium dichromate (50 g, mmol) and 500 cm^3 acetic acid were refluxed for 60 min. After the solvent was cooled to room temperature, the precipitate filter washed with water and dried. 6.1 g of yellow precipate was obtained (60.3 % yield). ^1H NMR ($CDCl_3$): δ = 7.69 (s, 4H), 4.07 (s, 12H). It is almost insoluble in benzene, acetic acid or ethanol, a bit in pyridine.

Synthesis of D: The active zinc powder (167 g, 2.6 mol) and **C** (10 g, 41.3 mmol) were added to a stirred aqueous solution (670 mL) of sodium hydroxide (50 g, 1.25 mol) under a N_2 atmosphere. The mixture was heated at 100 ^oC for 48 hours, and then cooled to room temperature. Concentrated hydrochloric acid (570 mL) was added. The reaction mixture was stirred for 1 h, and then filtrated. The solid was dried to give the pale-white pure compound **D** 7.3 g, yield 82.6 %, ^1H NMR ($CDCl_3$): δ = 8.03(s, 2H), 7.15(s, 4H), 4.04(s, 12H).

Synthesis of E: D was dissolved in boiling CCl_4 (100 mL). After cooling to room temperature, Br_2 (1.2 g, 0.38 mL, 7.5 mmol) was added via syringe .The mixture was heated (100 ^oC, bath temp) to a gentle boil when HBr start to evolve .The reaction was stopped after 35 min at reflux, the mixture

cooled and the precipitate filter and dried. The solid was cooked in toluene for another 30 min, then filter to give the brown pure **E**. ^{1}H NMR ($CDCl_3$): δ = 7.67 (s, 4H), 4.11 (s, 12H).

Synthesis of F: E and (3,5-bis(methoxycarbonyl)phenyl)boronic acid (mol/mol = 1:2.3), CsF and $Pd(PPh_3)_4$ were mixed in a two-necked shclenk flak and pumped for 30 minutes. 200 mL degassed $CH_3OCH_2CH_2OCH_3$ (DME) was added through a canula. The mixture was heated to reflux under N_2 for 48 hours. After the mixture was cooled to room temperature, water was added. The water phase was washed with $CHCl_3$. The mixed organic phases were dried with $MgSO_4$. After the solvent was removed, the crude product was purified by column chromatography (silica, $CHCl_3$) to give the pure product. ^{1}H NMR ($CDCl_3$): δ = 8.90 (t, 2H), 8.38 (d, 4H), 6.63 (s, 4H), 4.00 (s, 12H), 3.70 (s, 12H).

Synthesis of G: F (1.1 g, 1.58 mmol) was then suspended in a mixture of THF (20 mL) and MeOH (20 mL), to which 5 mL of 10 M NaOH aqueous solution was added. The mixture was stirred under reflux overnight and the THF and MeOH were removed under a vacuum. Dilute HCl was added to the remaining aqueous solution until the solution was at pH = 2. The solid was collected by filtration, washed with water and MeOH, and dried to give the yellow solid **F** (0.95 g, 96.3 % yield). ^{1}H NMR (400 MHz, DMSO): δ = 13.4 (s, 4H), 8.69 (t, 2H), 8.2 (d, 4H), 6.65 (s, 4H), 3.59 (s, 12H).

(3) Crystal structure date of 1, 2 and 3.

Table S1. Crystal data for **1-3**

Compound	**1**	**2**	**3**
Empirical formula	$C_{78}H_{66}N_2Ba_2O_{26}$	$C_{34}H_{34}BaO_{17}$	$C_{34}H_{24}BaO_{12}$
Formula weight	1722.01	851.95	761.89
Temperature/K	298(2)	298(2)	400(2)
Crystal system	triclinic	monoclinic	monoclinic
Space group	*P*-1	*C*2/c	*C*2/c
a/Å	9.0362(15)	32.24(5)	32.2746(7)
b/Å	17.484(3)	12.209(19)	12.6358(6)
c/Å	24.772(4)	8.885(13)	8.9507(2)
α/°	69.717(3)	90.00	90
β/°	84.873(3)	97.56(3)	98.533(2)
γ/°	82.904(3)	90.00	90
Volume/Å^3	3638.3(10)	3467(9)	3609.8(2)
Z	2	4	4
ρ_{calc}g/cm^3	1.481	1.494	1.402
μ/mm^{-1}	1.155	1.209	9.055
F(000)	1628.0	1560.0	1520
Reflections collected	18155	7731	12228
Independent reflections	12676[R_{int}=0.0291]	2978[R_{int}=0.1060]	3429 [R_{int}= 0.0485]
parameters	912	224	215
Goodness-of-fit on F^2	1.051	1.013	1.046
Final R indexes [I>=2σ (I)]	R_1 = 0.0834, wR_2 = 0.2099	R_1 = 0.0849, wR_2 = 0.2241	R_1 = 0.0604, wR_2 = 0.1625
Final R indexes [all data]	R_1 = 0.1012, wR_2 = 0.2193	R_1 = 0.1383, wR_2 = 0.2995	R_1 = 0.0718, wR_2 = 0.1801
Largest diff. peak/hole/ e Å^{-3}	7.99/-1.727	2.132/-3.457	2.243/-0.839
$R_1 = \Sigma\| \|F_o\|-\|F_c\| \| / \Sigma\|F_o\|$, $wR_2 = [\Sigma w(F_o^2-F_c^2)^2] / \Sigma w(F_o^2)^2]^{1/2}$			

(4) XRD spectrum of 1 and 2.

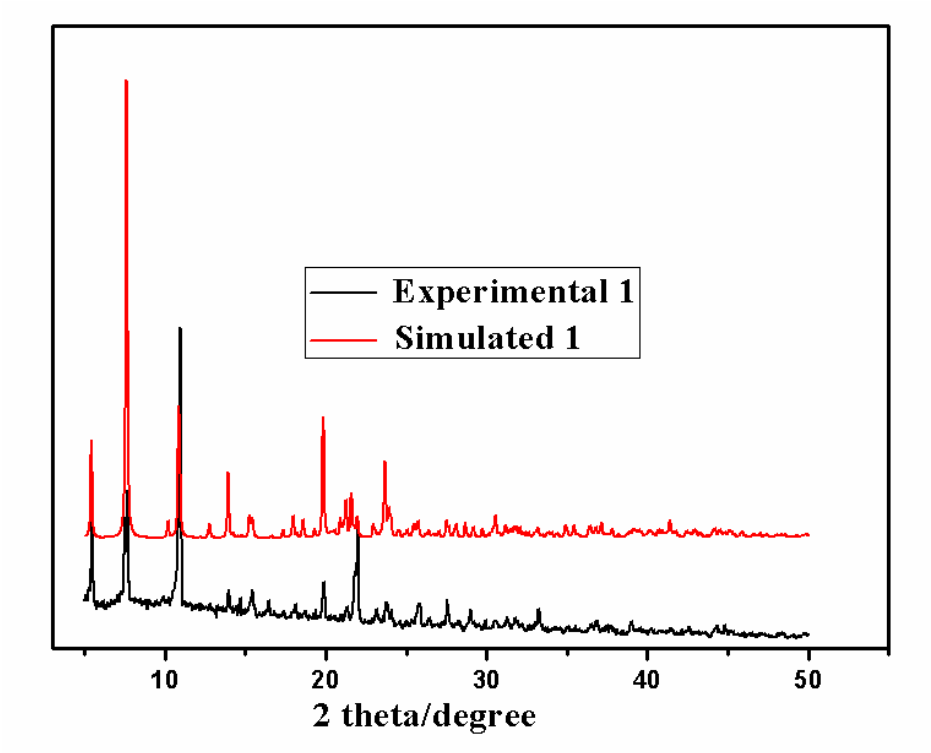

Figure S1. XRD spectrum of 1.

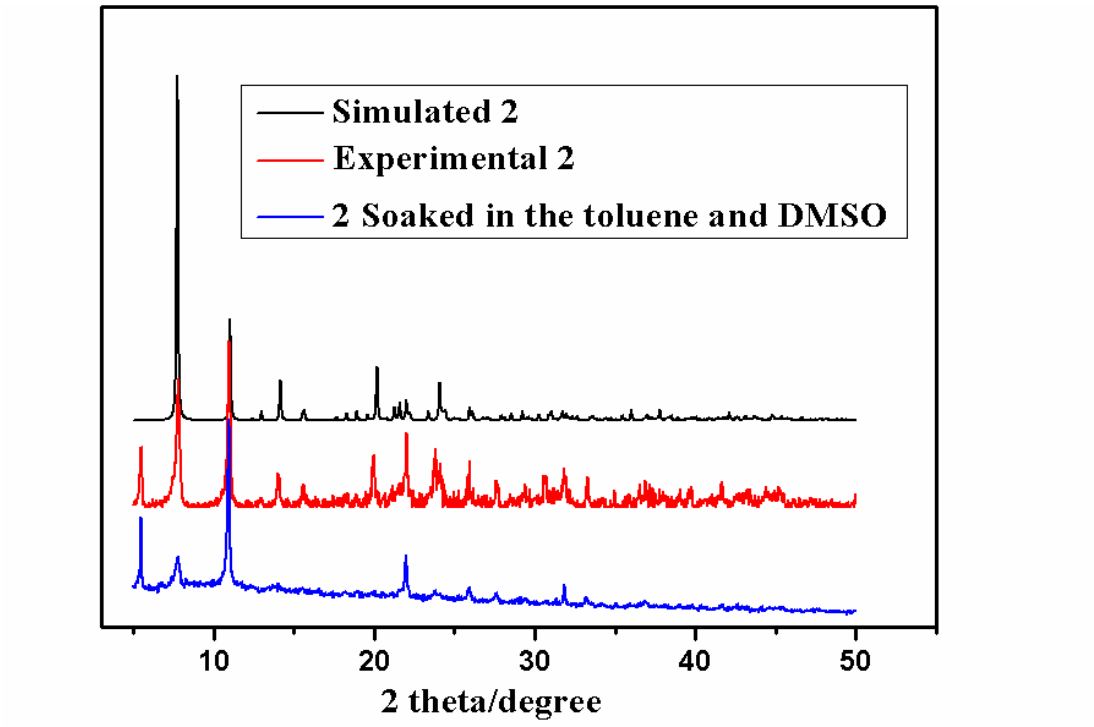

Figure S2. XRD spectrum of 2.

Note to the XRD of 2.

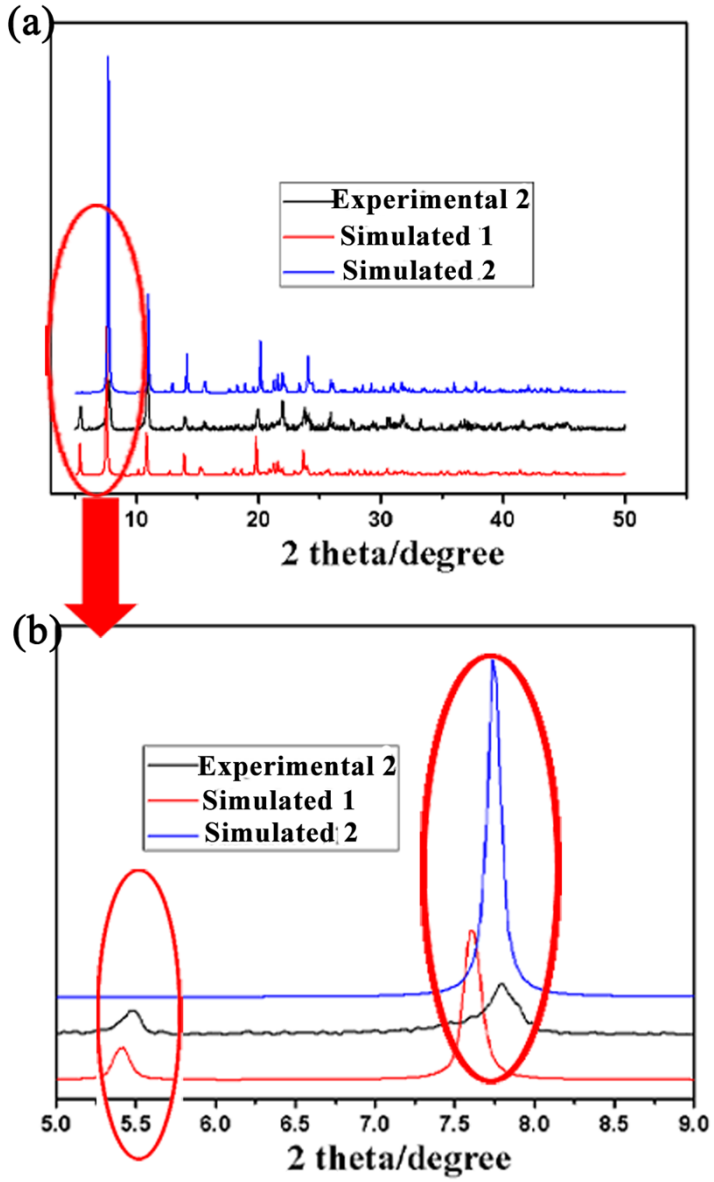

Figure S3. The comparison of XRD spectrum of 1 and 2.

Table S2. The unit cell of 2.

	a/Å	b/Å	c/Å	α/°	β/°	γ/°
1	32.24	12.00	9.00	90.00	98.36	90.00
2	32.13	12.25	8.98	90.00	98.48	90.00
3	33.65	12.81	9.26	90.00	98.07	90.00
4	33.07	12.66	9.17	90.00	98.09	90.00
5	32.63	12.18	8.99	90.00	98.17	90.00
6	32.39	12.24	8.97	90.00	98.17	90.00
7	32.51	12.58	8.86	90.00	98.56	90.00
8	32.50	12.30	9.00	90.00	98.78	90.00
9	32.48	12.22	8.96	90.00	98.28	90.00

The most obvious difference between XRD spectrum of **1** and **2** is whether the peak at 5.4° exists, and the other difference is a slight shift at 7.6°.

From the curve of experimental **2**, we found the existence of peak at 5.4°. We thought the compound **1** partly transform to **2**. However, the result of elemental analysis (Experimental Section) display the amount of nitrogen is 0, which indicate sample **2** is pure. Furthermore, we randomly selected some crystals from sample **2** and determined their unit cells, and matched well to the compound **2**'s unit cells (Table S2). From Figure. S3b, a slight shift between experimental **2** and simulated **1** indeed exist at 7.6°. Based on aforementioned evidences, we confirm the sample of **2** is pure.

(5) The TG curve of 1 and 2.

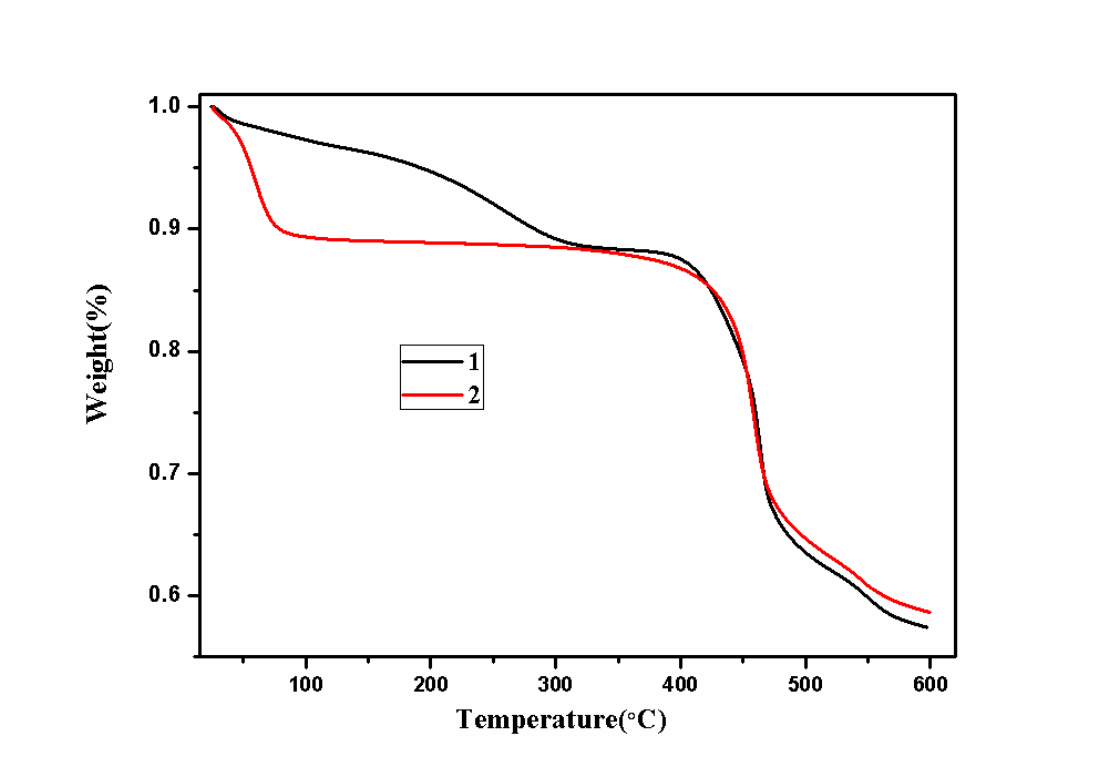

Figure S4. The TG curves of **1** and **2**. Thermogravimetric analysis (TGA) of **1** reveals that complex **1** can be stable up to 385 °C. The weight loss of 11.45 % from 30 to 325 °C corresponds to the loss of two NMP molecules (calcd: 11.49 %). For **2**, the weight loss of 10.8 % from 30 to 118 °C corresponds to the loss of five water molecules (calcd: 10.6%). There is no weight loss from 119 to 400 °C, and after 400 °C, **2** starts to decompose.

(6) The solid state photoluminescence of 1, 2 and H_4L^{OMe}.

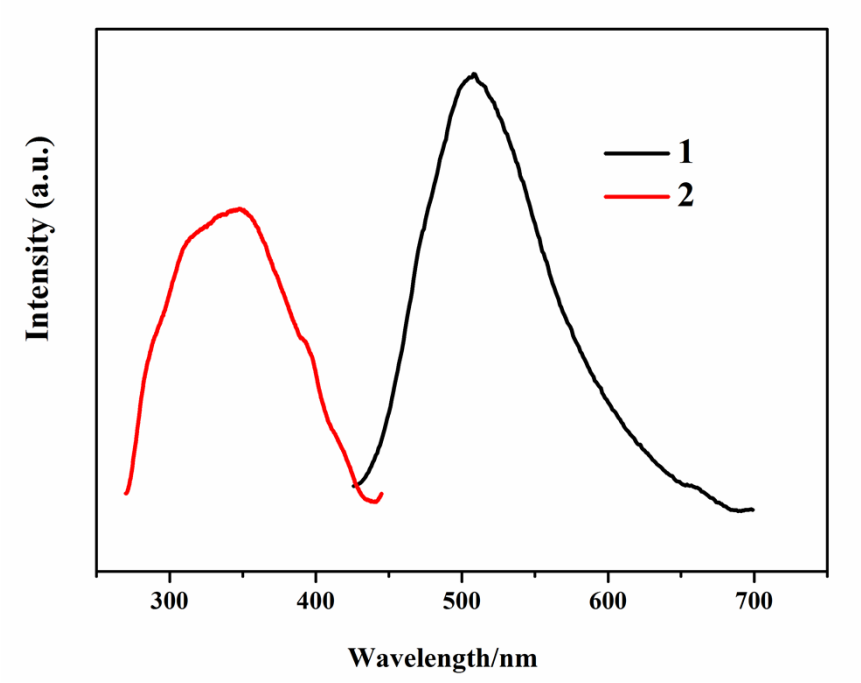

Figure S5. The solid state photoluminescence of **1** and **2** upon 360 nm and 230 nm excitation, respectively.

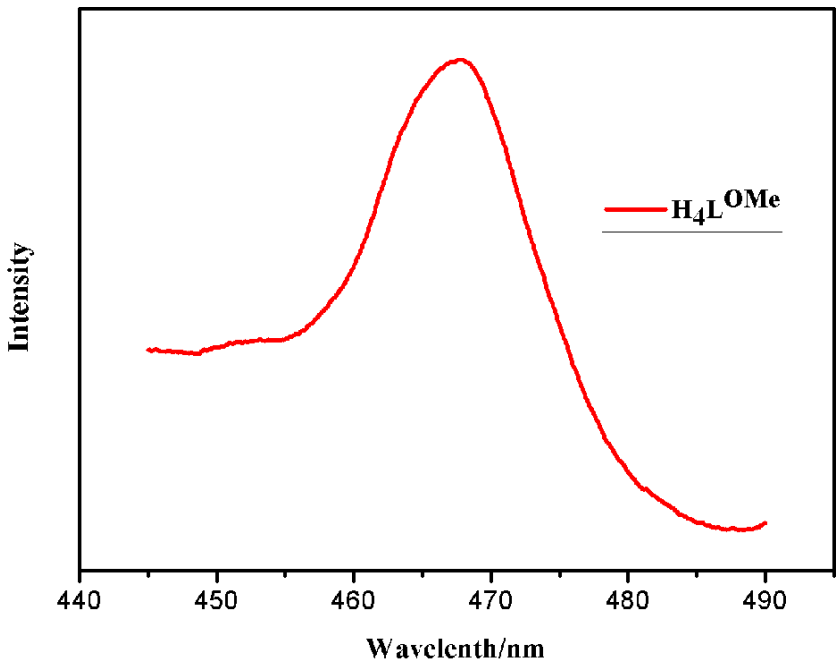

Figure S6. The solid state photoluminescence of of H_4L^{OMe} unpon 270 nm excitation.

(7) The gas adsorption of 3.

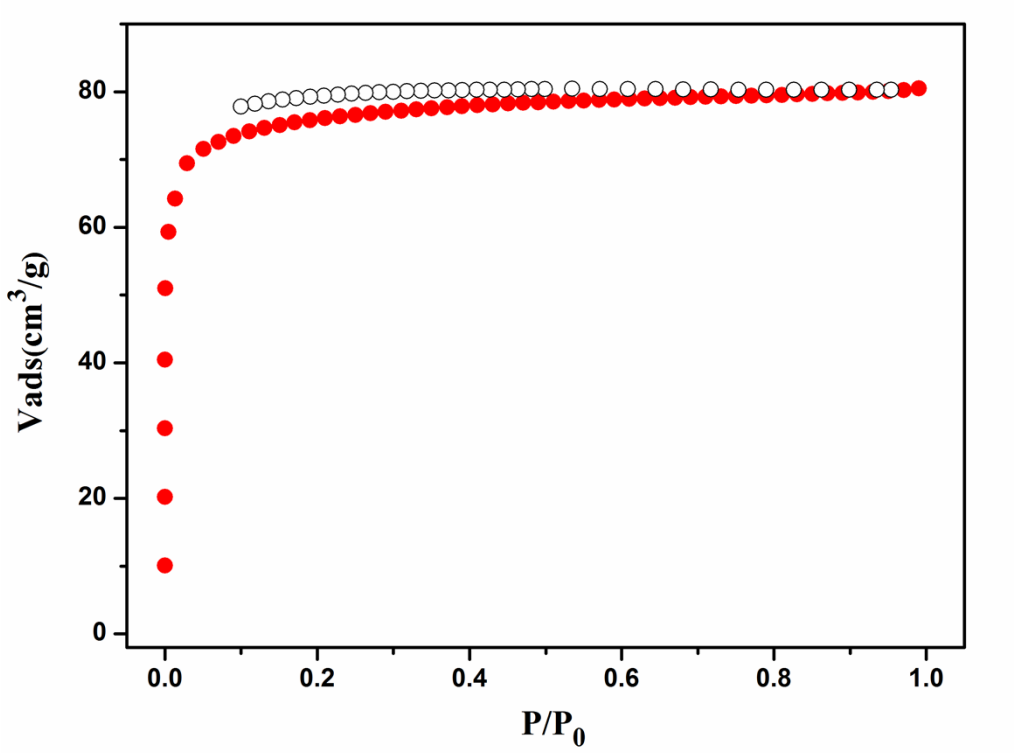

Figure S7. N_2 adsorption isotherms for **3**.

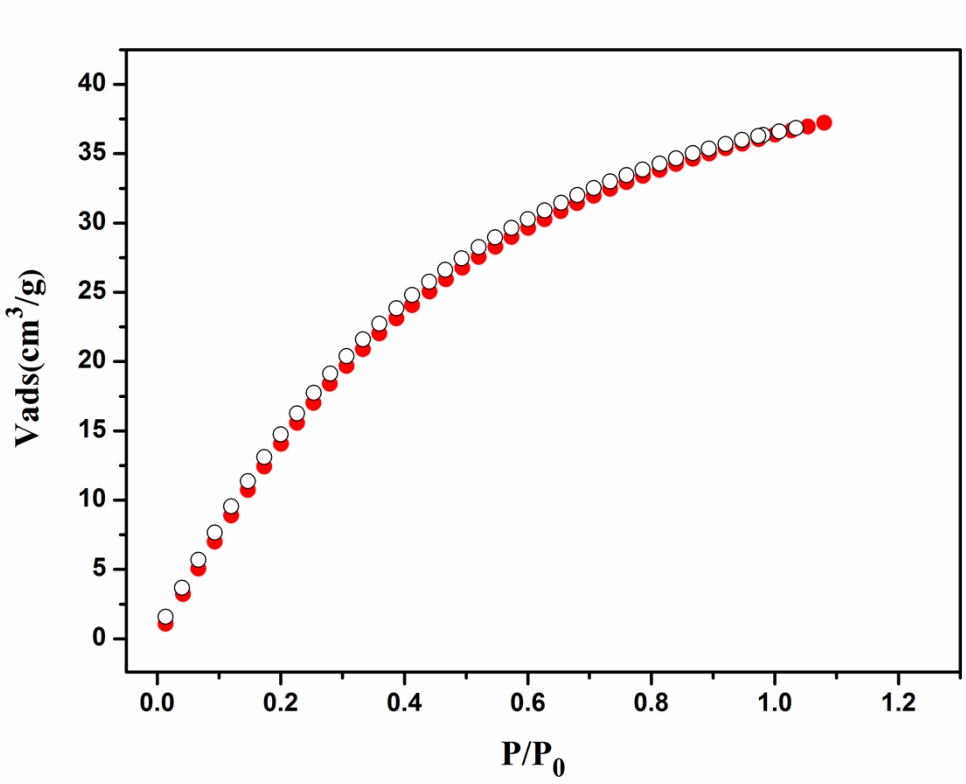

Figure S8. CO_2 adsorption isotherms for **3**.

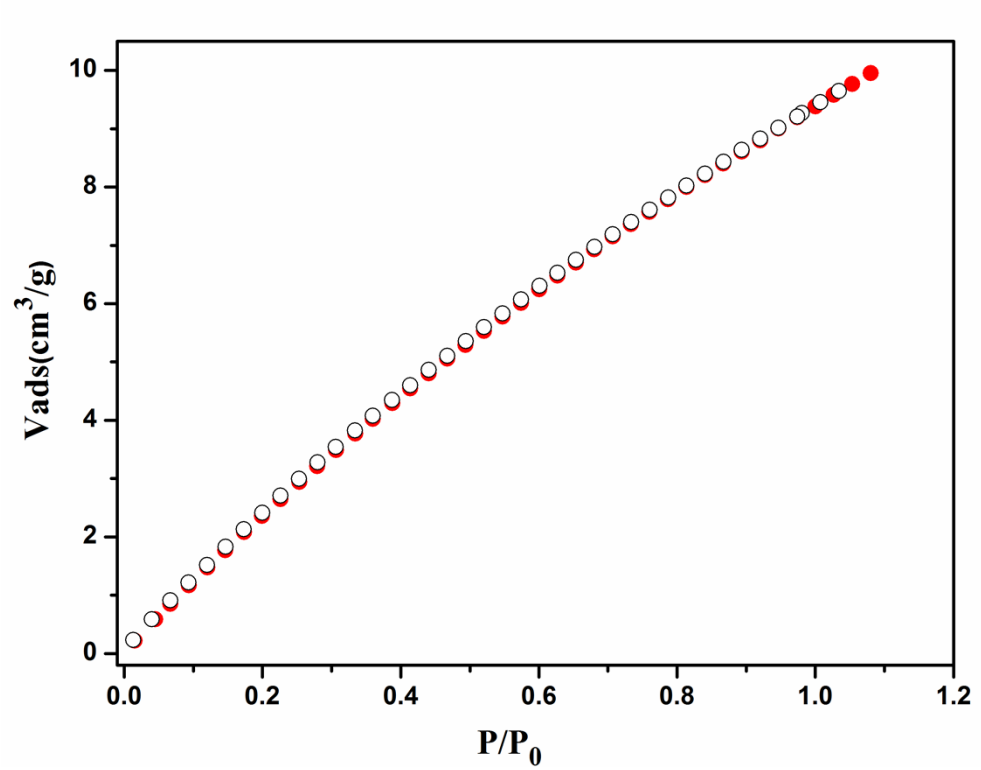

Figure S9. CH_4 adsorption isotherms for **3**.

(8) The catalytic properties of 3.

Cyanosilylation Reactions of aldehydes and ketones. The sample **2** was weighed before put into a shlenck tube . The tube was heated at 120 °C under dynamic vacuum for 2 h. After the tube was cooled to room temperature, aldehydes (2 mmol) or ketones (0.5 mmol) and trimethylsilyl cyanide (TMSCN) were added under N_2. The mixture was stirred at room temperature for two hours. After filtration, the aliquot of the liquid was dissolved in $CDCl_3$ and the ^1H NMR spectrum was recorded to evaluate the yield of aldehydes or ketones.

^{1}H NMR spectrum for reaction mixtures showing the conversion

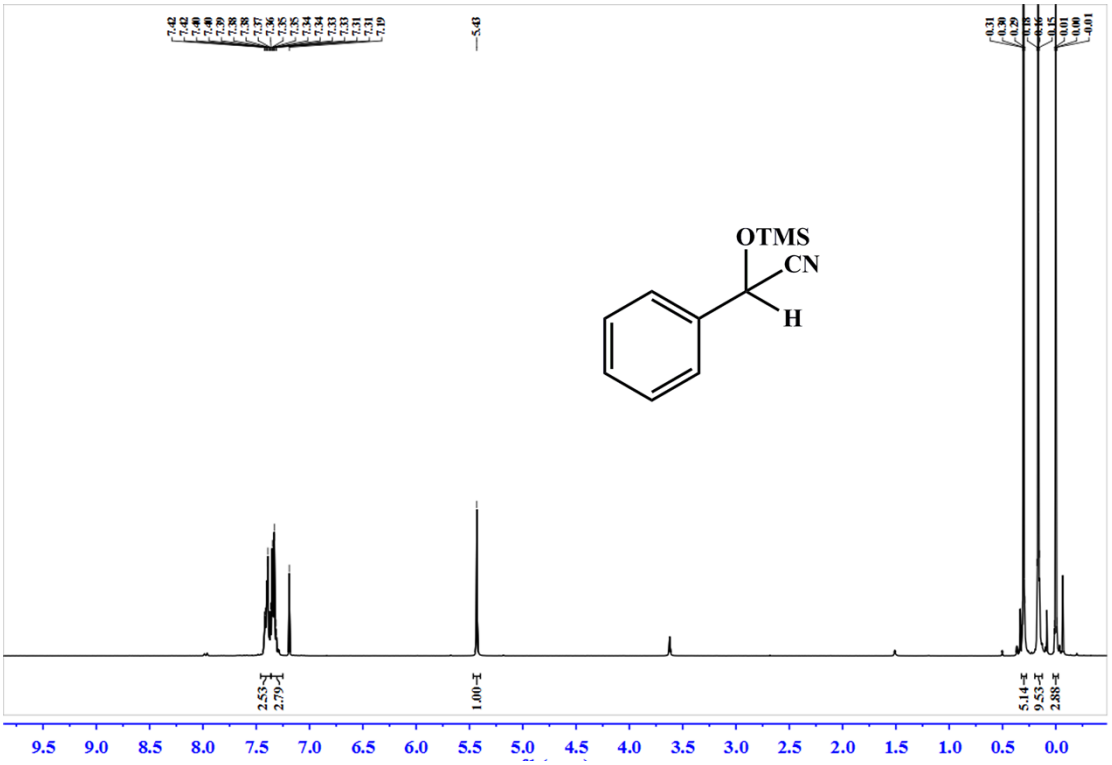

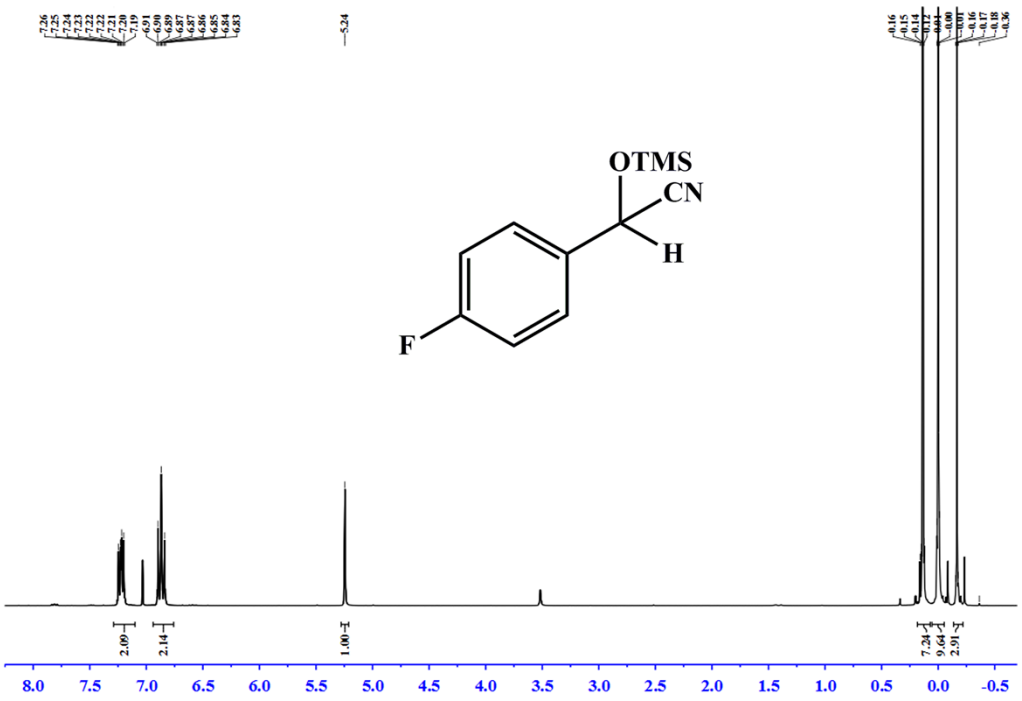
OTMS
CN
H
F
2.09
2.14
1.00
7.24
9.64
2.91
8.0 7.5 7.0 6.5 6.0 5.5 5.0 4.5 4.0 3.5 3.0 2.5 2.0 1.5 1.0 0.5 0.0 -0.5

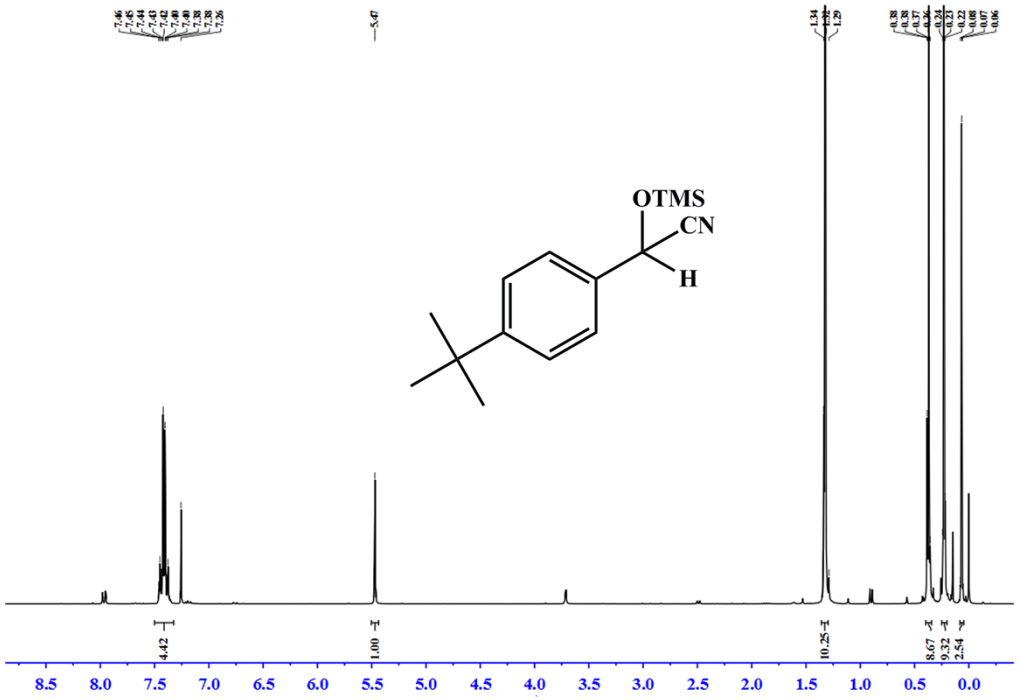
OTMS
CN
H
4.42
1.00
10.25
8.67
9.32
2.54
8.5 8.0 7.5 7.0 6.5 6.0 5.5 5.0 4.5 4.0 3.5 3.0 2.5 2.0 1.5 1.0 0.5 0.0

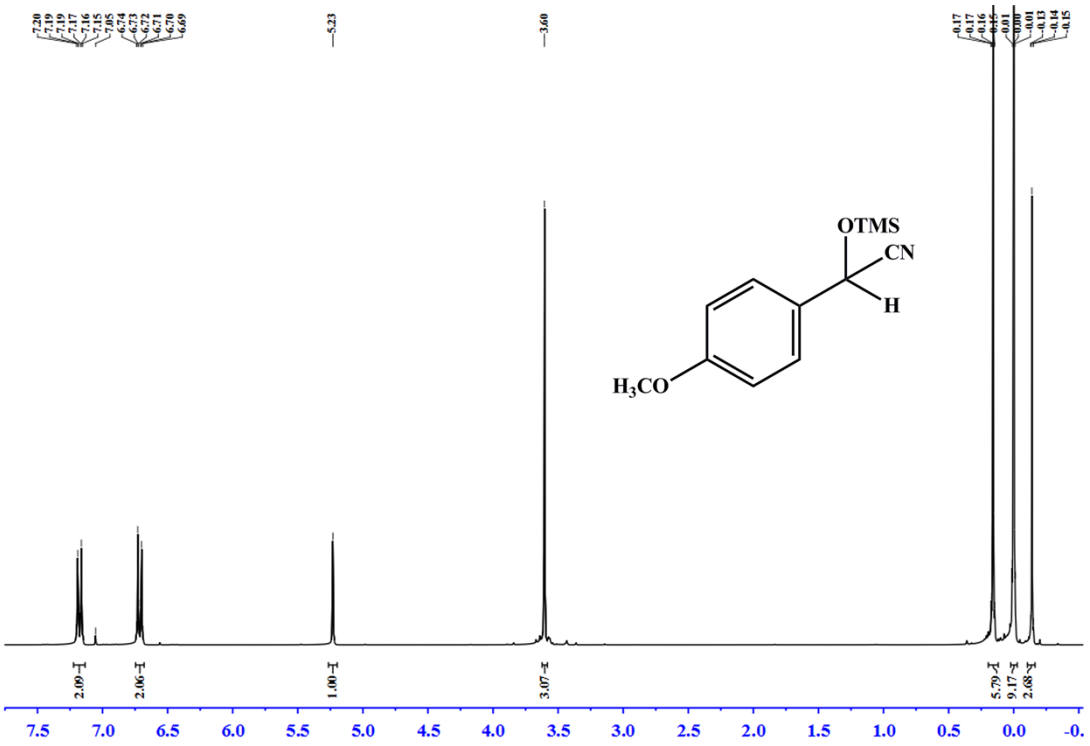
OTMS
CN
H
H3CO

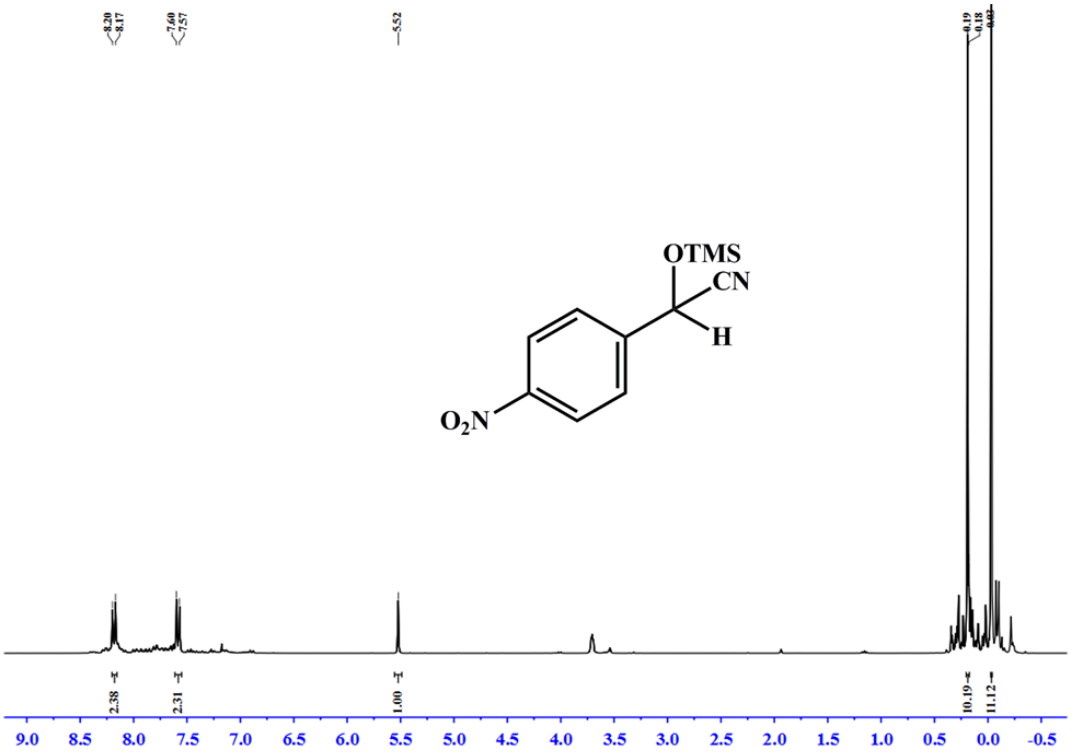
OTMS
CN
H
O2N

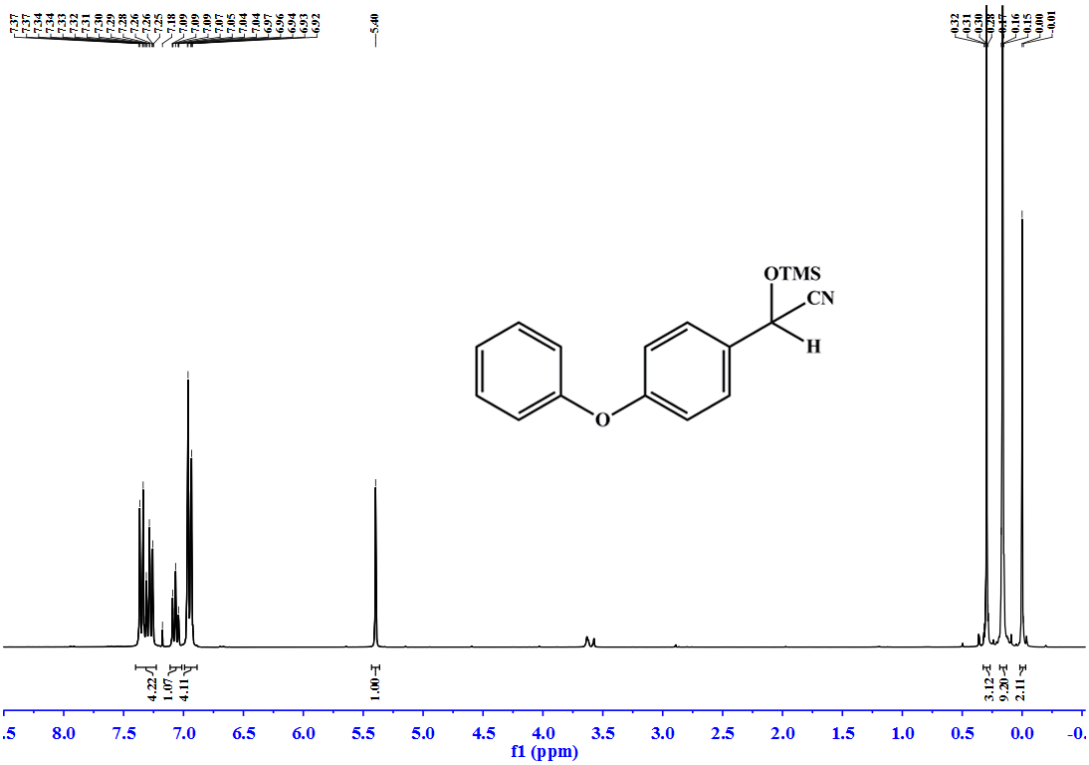
OTMS
CN
H
O
4.22
1.07
4.11
1.00
3.12
9.20
2.11
f1 (ppm)

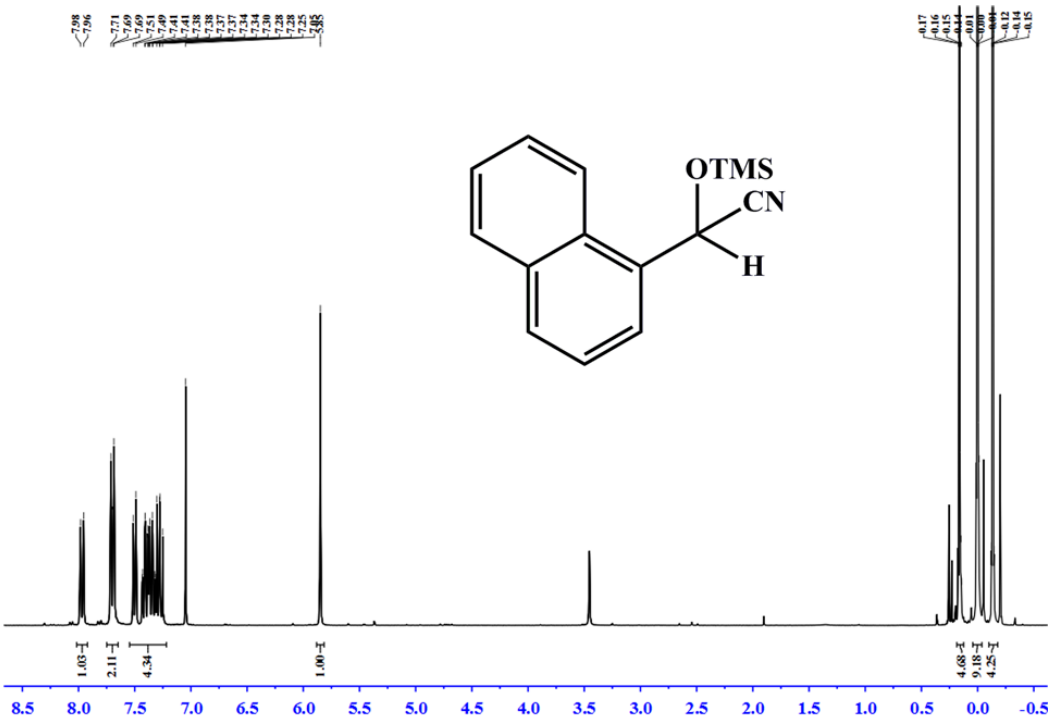
OTMS
CN
H
1.03
2.11
4.34
1.00
4.68
9.18
4.25

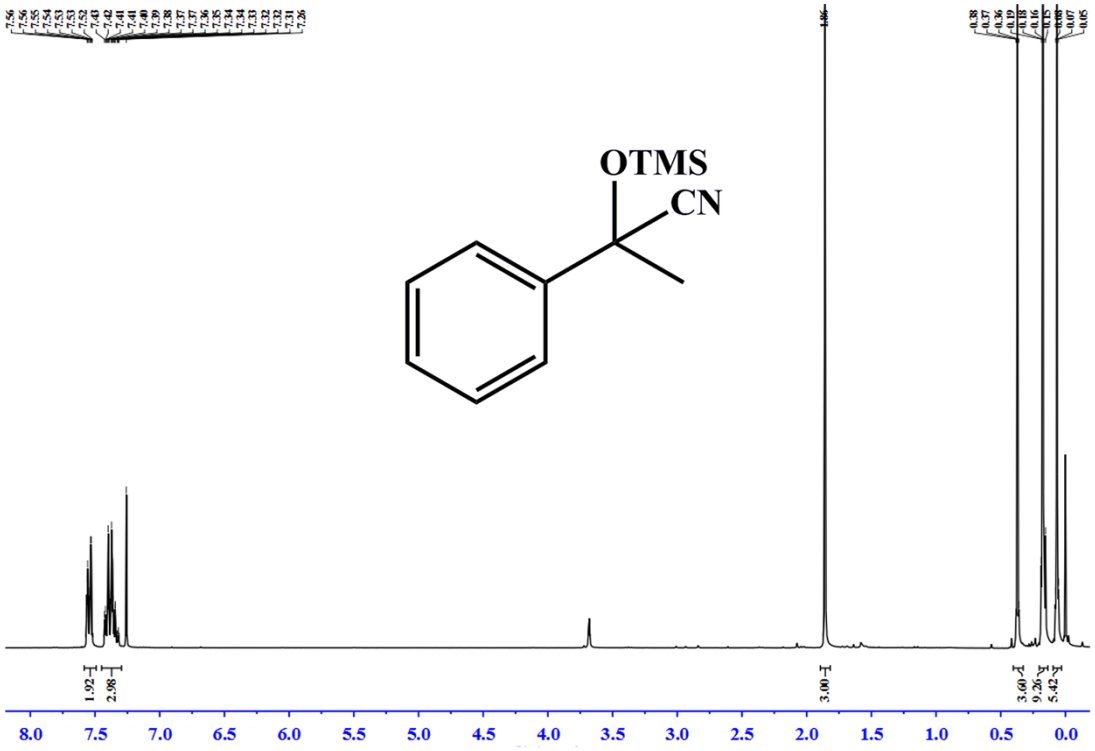
OTMS
CN
1.92
2.98
3.00
3.60
9.26
5.42
8.0
7.5
7.0
6.5
6.0
5.5
5.0
4.5
4.0
3.5
3.0
2.5
2.0
1.5
1.0
0.5
0.0

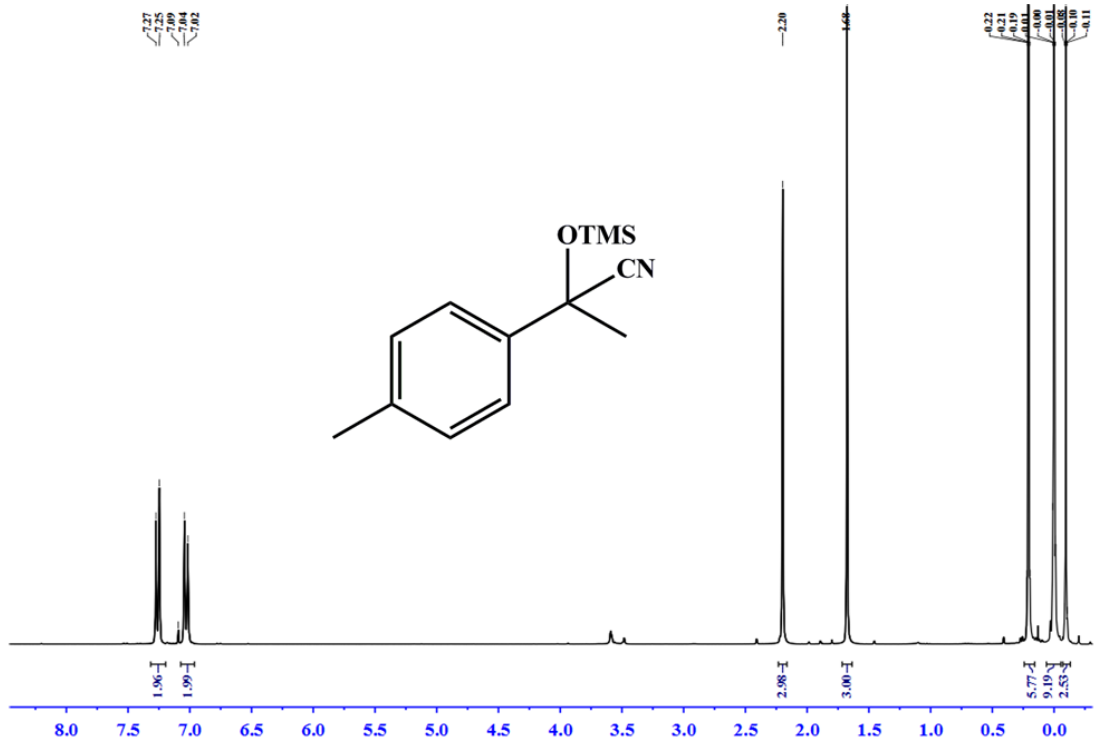
OTMS
CN
1.96
1.99
2.08
3.00
5.77
9.19
2.53
8.0
7.5
7.0
6.5
6.0
5.5
5.0
4.5
4.0
3.5
3.0
2.5
2.0
1.5
1.0
0.5
0.0

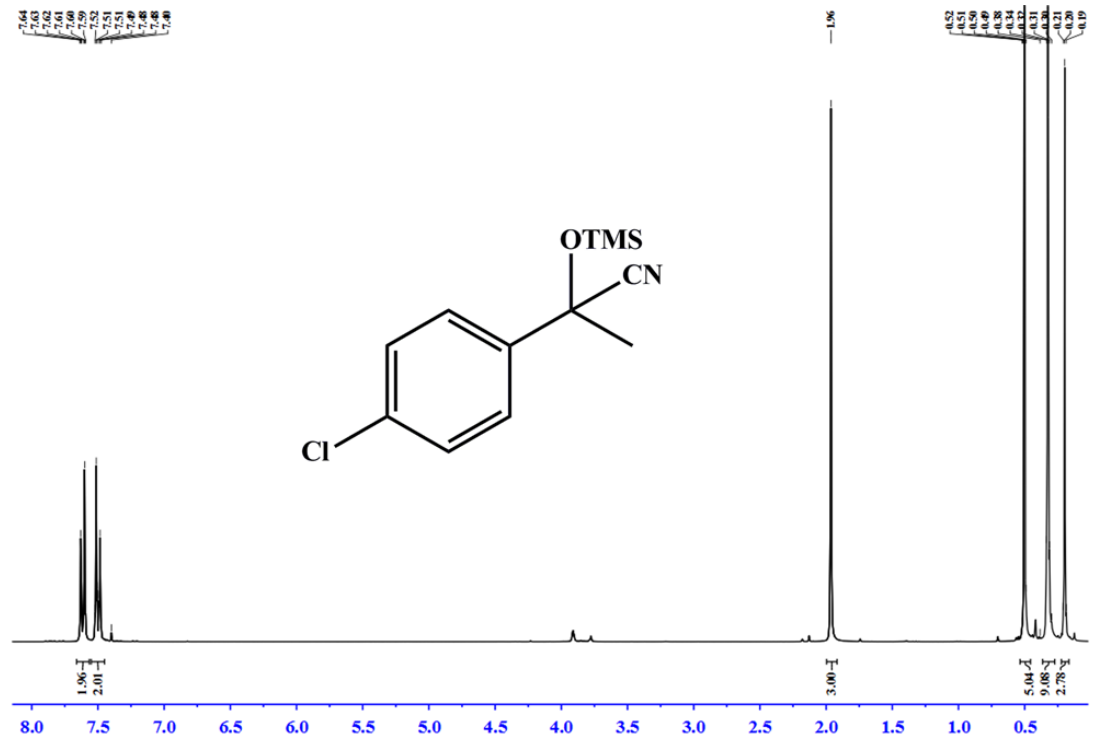
OTMS
CN
Cl
8.0 7.5 7.0 6.5 6.0 5.5 5.0 4.5 4.0 3.5 3.0 2.5 2.0 1.5 1.0 0.5

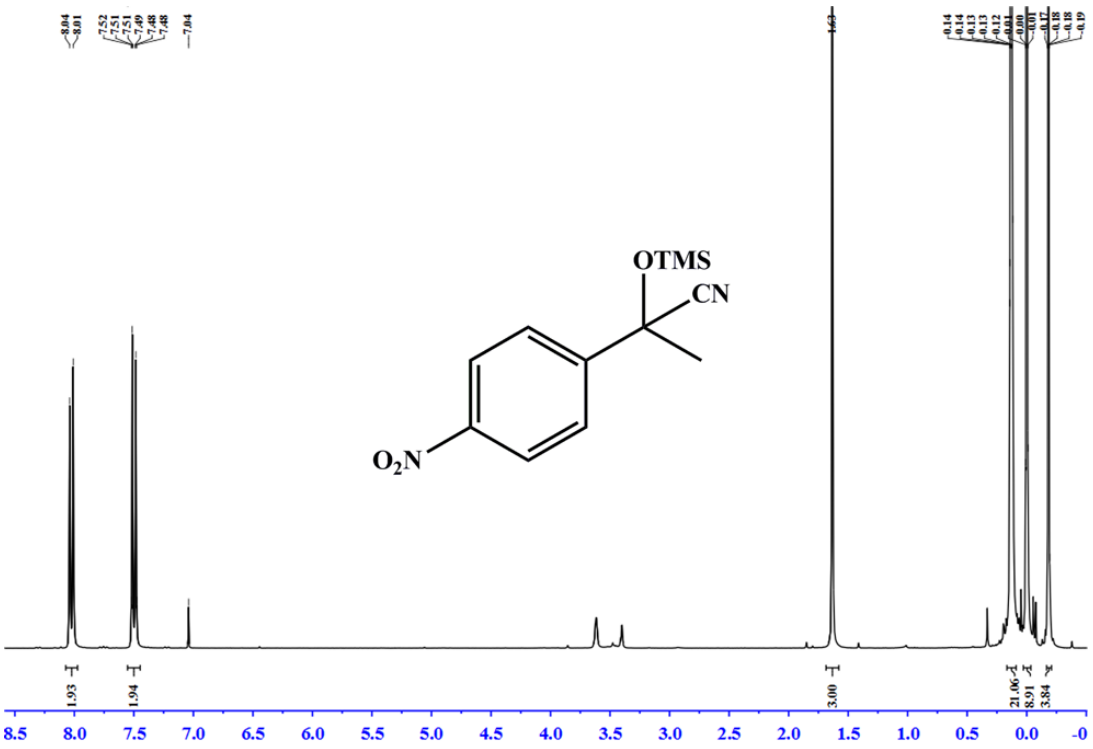
OTMS
CN
O_2N
8.5 8.0 7.5 7.0 6.5 6.0 5.5 5.0 4.5 4.0 3.5 3.0 2.5 2.0 1.5 1.0 0.5 0.0 -0

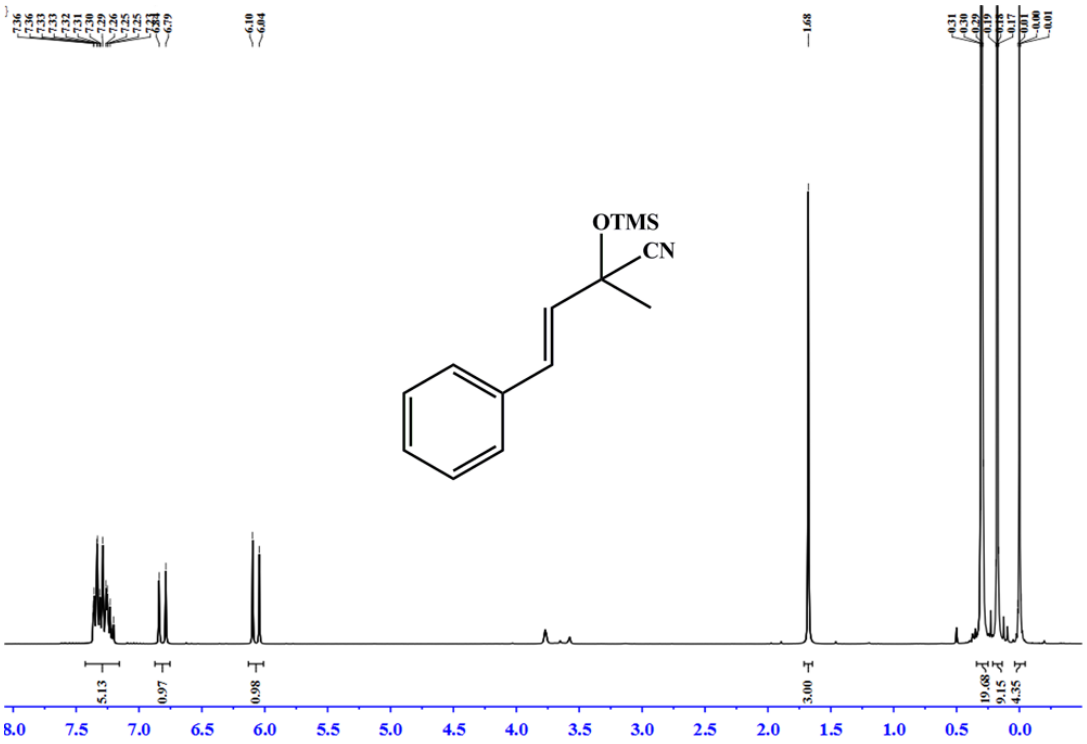
OTMS
CN
5.13
0.97
0.98
3.00
19.68
9.15
4.35
8.0 7.5 7.0 6.5 6.0 5.5 5.0 4.5 4.0 3.5 3.0 2.5 2.0 1.5 1.0 0.5 0.0

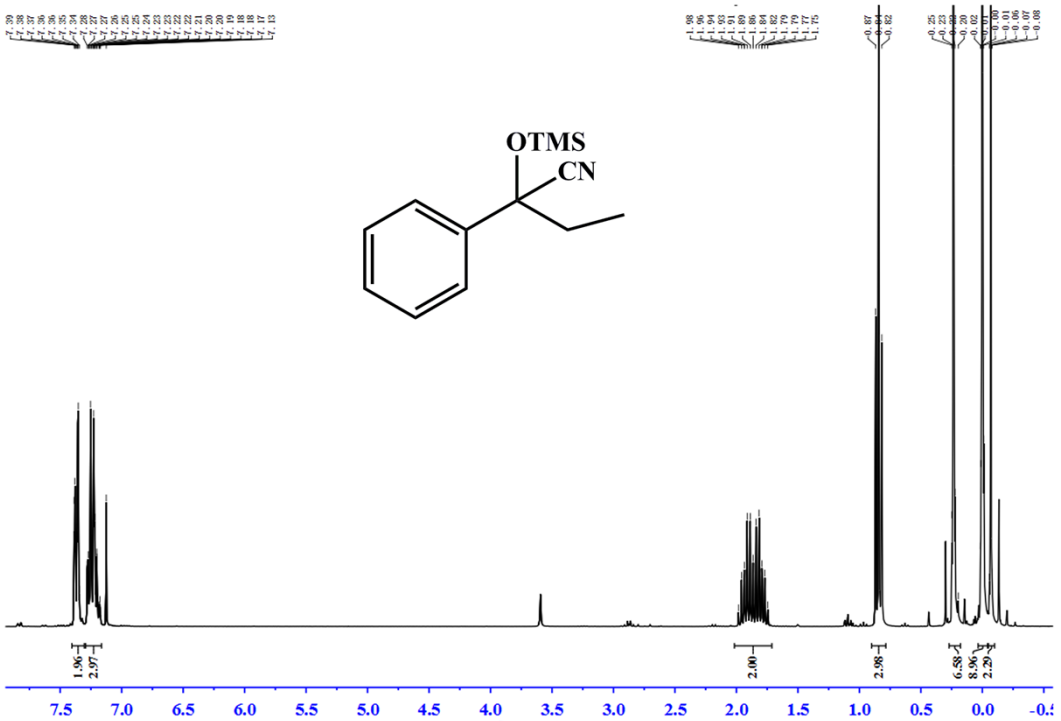
OTMS
CN
1.96
2.97
2.00
2.98
6.58
8.96
2.29
7.5 7.0 6.5 6.0 5.5 5.0 4.5 4.0 3.5 3.0 2.5 2.0 1.5 1.0 0.5 0.0

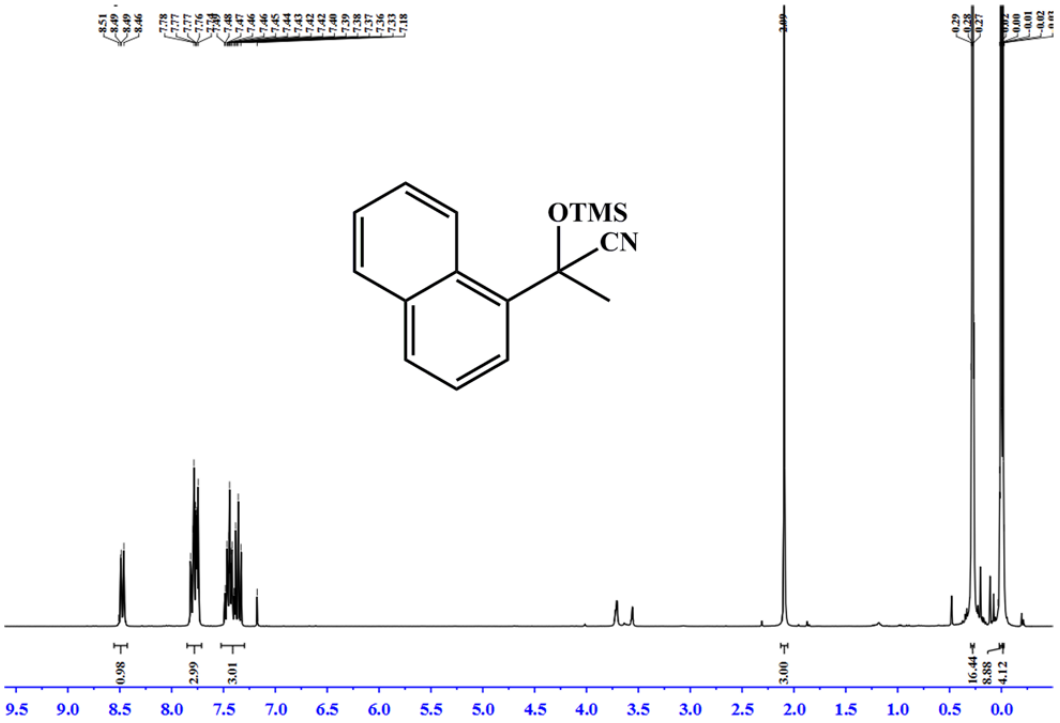

Discussion on the Catalytic Activity. To compare the catalytic activity of compound **3** with those of known MOFs, the reported results are summarized in Table S2. Because the reaction conditions are different in each literature, the comparison of the yields is not appropriate. Therefore, we have calculated the TON and TOF values for the comparison. The large TON and TOF values calculated for **3** strongly indicate the high activity of this material.

Table S3 Comparison of the catalytic activity of MOFs in cyanosilylation reactions of benzaldehyde.

catalyst	mol % cat	molar ratioa	solvent	T /°C	T /h	yield (%)	TON[b]	TOF[c] /h−1	ref
3	0.5	1:2	neat	r.t.	0.5	96	192	384	this work
Sc-MOF	2	1:2	neat	40	12	90	45	3.75	1
$[Zn_3(bpy)_{3.5}(\mu\text{-}O_2CH)_4(ClO_4)_2]_\infty$	13	1:2	CH_2Cl_2	r.t.	24	22	1.7	0.07	2
MIL-101(Cr)	1	1:2	heptane	40	3	98	98	33	3
CPO-27-Mn	10	1:2	CH_2Cl_2	40	1	100	10	10	4
Ce-MDIP1	2	1:2.4	CH_3CN	r.t.	11	100	50	4.5	5
RPF-21-Pr	1	1:1.5	neat	40	4	90.7	90.7	22.7	6
RPF-22-Pr	1	1:1.5	neat	40	6	10.2	10.2	1.7	6
RPF-23-Pr	1	1:1.5	neat	40	6	13.8	13.8	2.3	6
RPF-21-La	1	1:1.5	neat	40	4	93.2	93.2	23.3	6
RPF-21-Nd	1	1:1.5	neat	40	4	89.2	89.2	22.3	6

$[Fe_2Ag_2(pca)_4(pcaH)(MeOH)_2](ClO_4)_2 \cdot 3MeOH$	1.7	1:2	CH_2Cl_2	25	3	51	30	10	7
POMOF-1	1	1:2.4	CH_3CN	r.t.	24	98.1	98.1	4	8
La-BTTc	1	1:1	neat	r.t.	2	82	82	41	9
La-BTTc	1	1:1	neat	r.t.	0.5	68	68	134	9
$Mn_3[(Mn_4Cl)_3(BTT)_8(CH_3OH)_{10}]_2$	11	1:2	CH_2Cl_2	r.t.	9	98	8.9	0.99	10
La-TTTA	2.5	1:2	neat	r.t.	2	99.7	39.88	19.94	11
Nd-TTTA	2.5	1:2	neat	r.t.	2	98.32	39.33	19.66	11
$Cu(BrDPMP)_2$	2	1:1.2	THF	r.t.	2	80	40	20	12
Cu-DDQ	2.5	1:2	neat	r.t.	1	95	38	38	13
$[Zn_3(TCPB)_2]\infty$	2.5	1:2	hexane	r.t.	13	100	40	3.1	14
CoNiBpe-2	10	1:5	neat	80	16	77	7.7	0.48	15
Nd(btc)-MOFs	4.5	1:2	CH_2Cl_2	r.t.	2	99	22	11	16
(O_2H_3)Sc-MOF	5	1:1.5	neat	40	8	84	16.8	2.1	17
$(\mu\text{-}OH)_6$Sc-MOF	5	1:1.5	neat	40	8.5	77.3	15.46	1.9	17
(Phen)Sc-MOF	5	1:1.5	neat	40	7	55	11	1.6	17
RPF-18-Pr	5	1:1.5	neat	50	3	77.8	15.56	5.2	18
RPF-18-La	5	1:1.5	neat	50	2	85.7	17.14	8.57	18
RPF-19-Nd	5	1:1.5	neat	50	2	94.8	18.96	9.48	18
(R)-1-Li	0.5	1:1	toluene	-78	0.75	97	194	258.7	19

[a]PhCHO:TMSCN. [b]TON = (yield)/(mol % cat). [c]TOF = (TON)/(t).

Recycling Experiment. The reuse experiment was carried out for the cyanosilylation of benzaldehyde. The reaction was carried out under the standard conditions. After the reaction was completed, the catalyst was recovered by filtration, washed with CH_2Cl_2, and reactivated prior to being used for the reuse experiment. In addition, the recovered catalyst can be reused for cyanosilylation of benzaldehyde without any loss of its high catalytic performance.

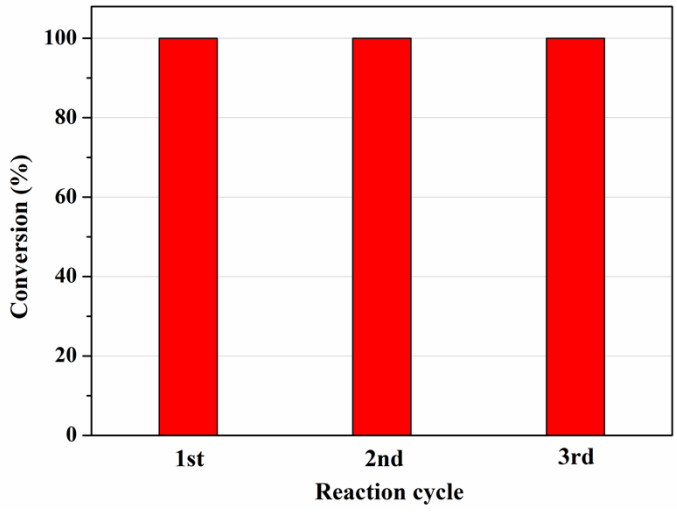

Figure S10. Recycling tests for cyanosilylation of benzaldehyde catalyzed by **3**.

Cycloaddition of epoxide and CO_2. All syntheses were carried out in a 20 mL stainless steel reactor equipped with a magnetic stirrer, which was charged with epoxide (15.0 mmol), catalyst (amount indicated in the text), and then CO_2 (initial pressure indicated in the text). The mixture was heated to 80 °C from room temperature in 40 minutes, kept at 80 °C for 4 hours. The reactor was then cooled in an ice bath, and excess CO_2 was released carefully. The filtrate was subsequently analyzed using gas chromatography to determine conversion, selectivity, and yield.

Table S4 Comparison of the catalytic activity of MOFs in cycloaddition of CO_2 and styrene oxide.

catalyst	mol % cat	co-catalyst	P_{CO2} (MPa)	T /°C	T /h	yield (%)	TON	TOF /h^{-1}	ref
3	0.133	TBAB	0.6	80	4	80	601.5	150.4	this work
CHB(M)	1.6	none	1.2	120	6	56.25	35.16	5.86	20
MOF-5	0.7	TBAB	0.1	50	15	92	131.4	8.7	21
gea-MOF-1	0.15	TBAB	2	120	6	85	567	94	23
Ni(salphen)-MOF	0.28	TBAB	2	80	4	81	289.3	72.3	24
MIL-68 (In)	9.65	none	0.8	150	8	42	4.352	0.544	25
MIL-68(In)-NH_2	8.7	none	0.8	150	8	74	8.472	1.059	25
BIT-103	0.4	none	3	160	24	94.47	236	9.8	26
(salen)Cr(III)	1	DMAP	0.3	85	7	99	99	14.1	27

Table S5 Comparison of the catalytic activity of MOFs in cycloaddition of CO_2 and 2-(phenoxymethyl)oxirane.

catalyst	mol % cat	co-catalyst	P_{CO2} (MPa)	T /°C	T /h	yield (%)	TON	TOF /h^{-1}	ref
Compound **3**	0.133	TBAB	0.6	80	4	98	736.8	184.2	this work
CHB(M)	1.6	none	1.2	120	6	71.05	44.4	7.4	20
MOF-5	0.7	TBAB	0.1	50	1	56	80	26.7	21
MOF-5	0.7	TBAB	6	50	4	97	138.6	34.6	21
MMCF-2	0.125	TBAB	0.1	R.T.	48	37.6	300.8	6.3	22
Ni(salphen)-MOF	0.28	TBAB	2	80	4	55	196.4	49.1	24
Ni(salphen)-MOF	0.28	TBAB	2	80	24	82	292.8	12.2	24
BIT-103	0.4	none	3	160	24	98.6	238	9.9	26

Computational model and method

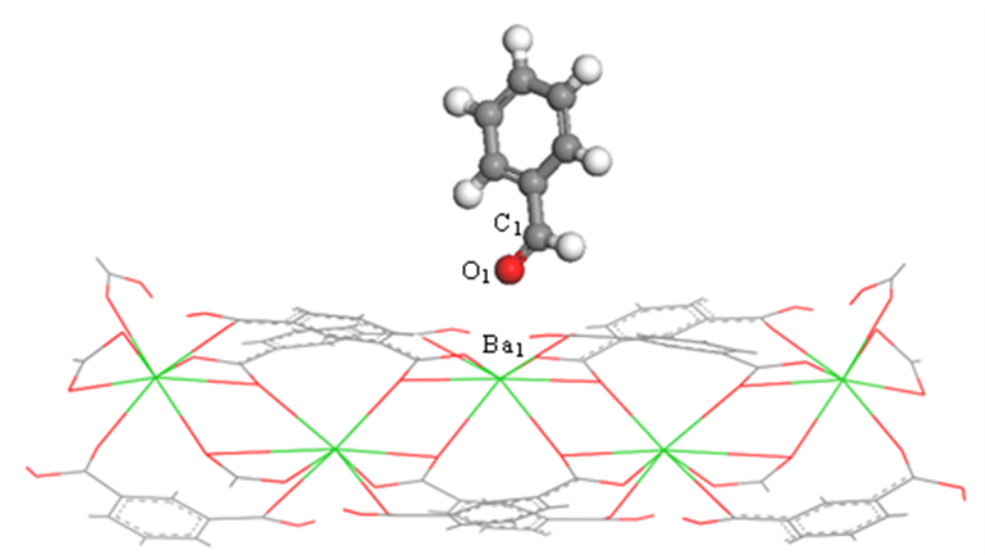

Figure S11. The optimized structure of the C_6H_5CHO molecule adsorbed on the cluster of Ba-MOF. (Ba, green; O, red; C, gray; H, white).

Density functional theory (DFT) calculations were performed with the program package DMol^3 in Materials Studio of Accelrys Inc[27-29]. The exchange correlation energy was calculated with the generalized gradient approximation (GGA) using the form of functional proposed by Perdew and Wang[30,31], usually referred to as Perdew-Wang 91 (PW91). To take the relativity effect into account, the density functional semicore pseudopotential (DSPP)[32] method was employed for the Ba atoms, and the carbon, oxygen, and hydrogen atoms were treated with an all-electron basis set. The valence electron functions were expanded into a set of numerical atomic orbital by a double-numerical basis with polarization functions (DNP). Fermi smearing of 0.005 hartree and a realspace cutoff of 5.2 Å were used to improve the computational performance. The tolerances of energy, gradient, and displacement convergence were 2×10^{-5} hartree, 4×10^{-3} hartree/Å, and 5×10^{-3} Å, respectively. All computations were performed with spin polarization.

The Ba-MOF cluster model was selected to represent complex **3** structures in this work. The cluster model is a common method widely used in zeolitesand MOFs[33-36]. The Ba-MOF cluster model was extracted from the experimental crystal structure of complex **3**. As shown in Figure S11, in the cluster model, five Ba metal atoms and eight surrounding $H_4\mathbf{L}^{OMe}$ ligands

were included. The boundary metal and carbon atoms, which bond to the next ligand in the periodic structure, were saturated with formate and proton, respectively.

Natural bond orbital (NBO) analysis was performed on theoptimized structure of each complex to determine the NBO charges on various atoms involved in complexation. The NBO analysis developed by Reed *etal*.[37] to study orbital interactions is a reliable tool for therationalization of chemical bonds. The NBO population analysis was performed using the Becke three-parameter hybrid (B3LYP[38,39]) method in conjunction with the basis set of 6-31G(d) for C, H, and O and Stuttgart-Dresden (SDD) relativistic effective core potential for Ba [40-42]. All of the calculations were carried out using the NBO 3.1 program implemented in Gaussian 09[43].

Table S6 Geometry parameters of Ba-MOF, C_6H_5CHO, and C_6H_5CHO-Ba-MOF complex (unit of Å)

parameters	Ba-MOF	C_6H_5CHO	complex
C_1-O_1		1.222	1.230
Ba_1-O_1			2.910
Ba_1-O	2.841		2.878

(9) The sensing of small molecules by 1 and 2

The as-synthesized sample of **1** (8.0 mg) and **2** (4.0 mg) was ground and suspended in toluene solution (5 ml), to which was dropwise added different organic molecules (DMSO, DMF, methanol, ethanol, 1-propanol, 2-propanol, hexane, acetone, dichloromethane, THF, acetonitrile).

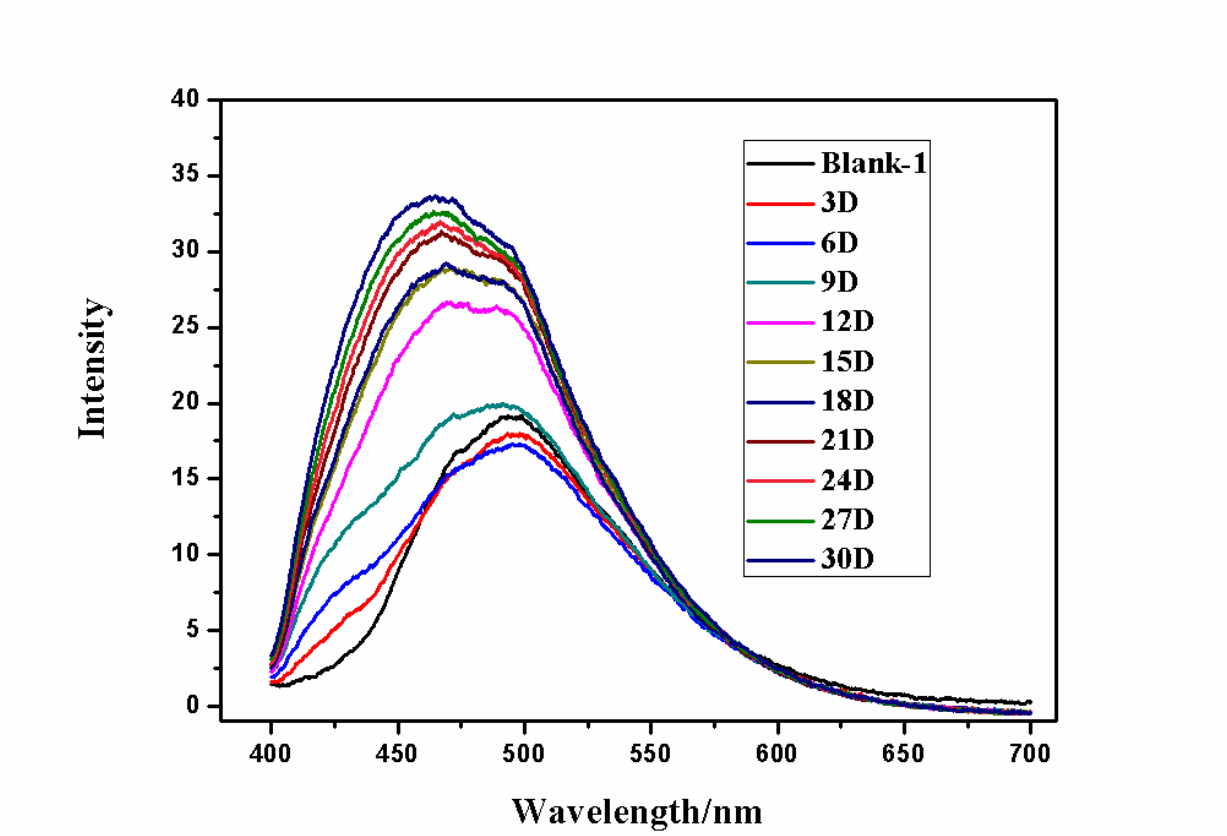

Figure S12. Emission spectra of an emulsion of **1** in 5ml toluene in the presence of different concentrations of DMSO (excited at 380 nm).

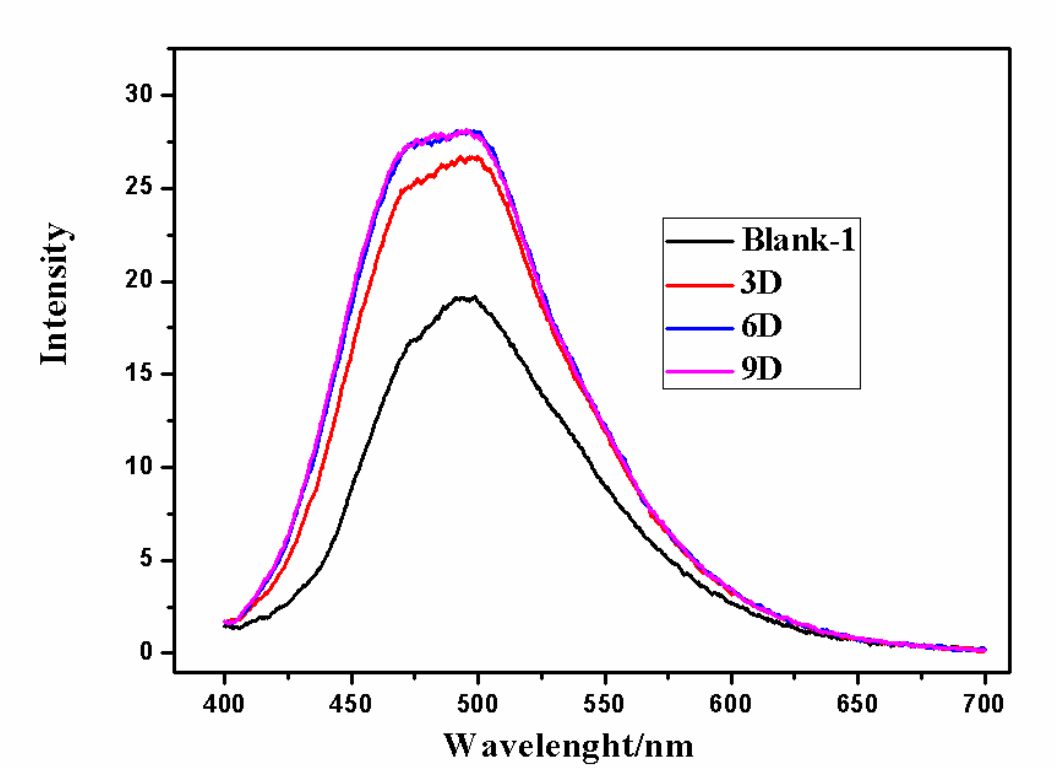

Figure S13. Emission spectra of an emulsion of **1** in 5ml toluene in the presence of different concentrations of DMF (excited at 380 nm).

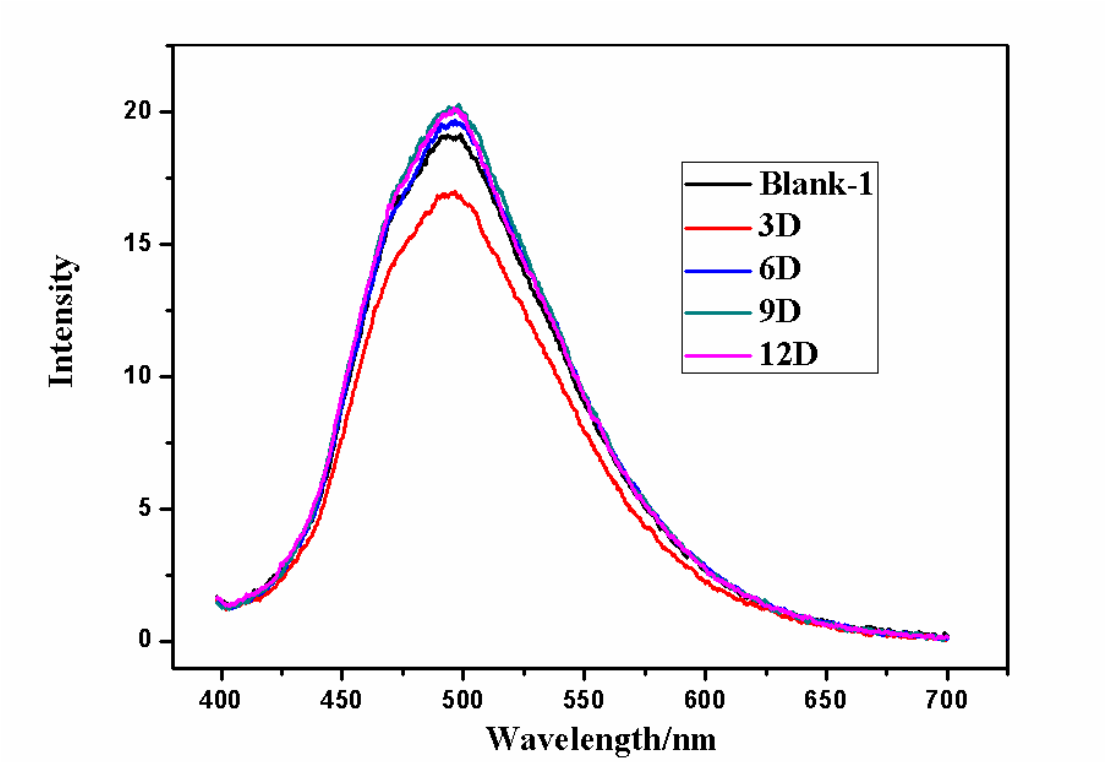

Figure S14. Emission spectra of an emulsion of **1** in 5ml toluene in the presence of different concentrations of THF (excited at 380 nm).

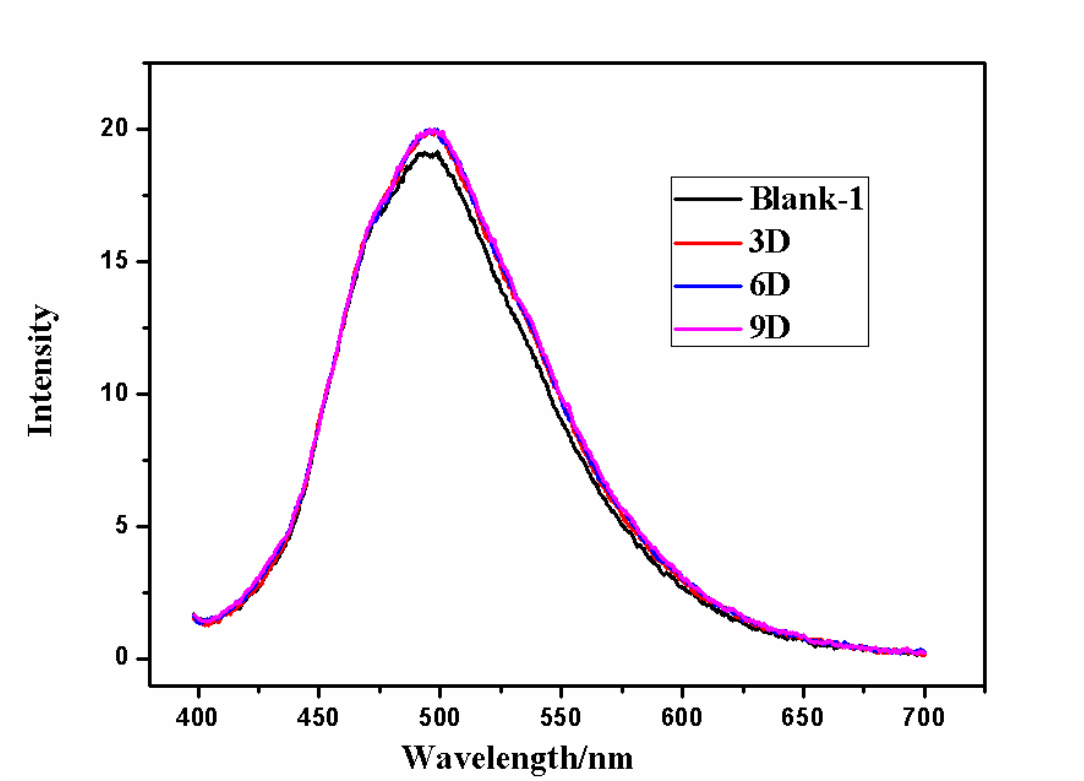

Figure S15. Emission spectra of an emulsion of **1** in 5ml toluene in the presence of different concentrations of acetone (excited at 380 nm).

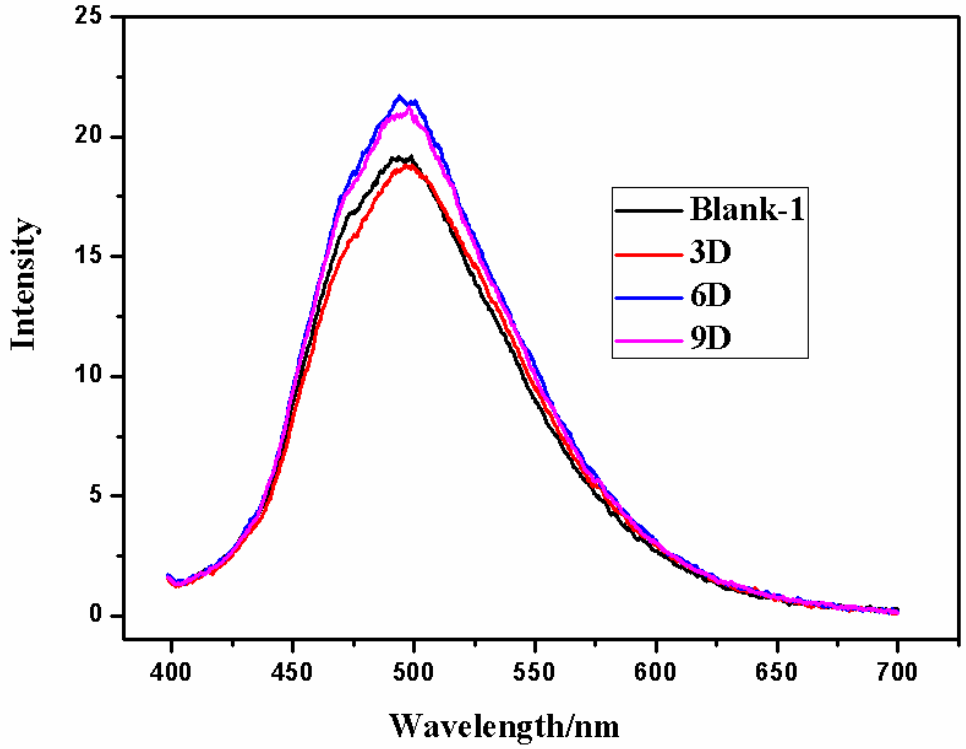

Figure S16. Emission spectra of an emulsion of **1** in 5ml toluene in the presence of different concentrations of dichloromethane (excited at 380 nm).

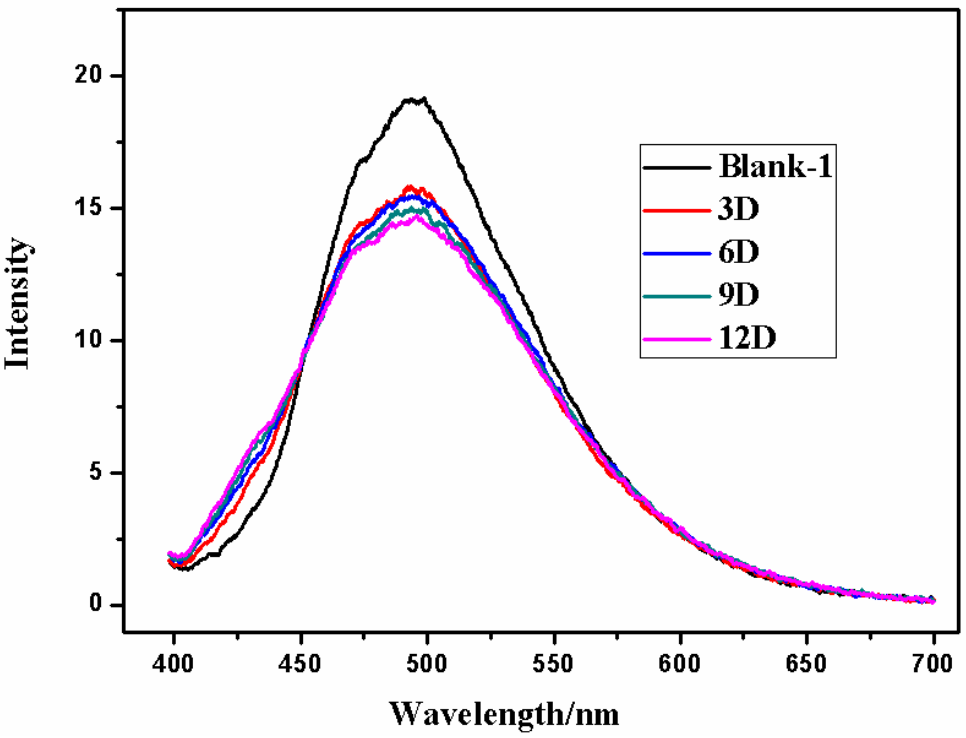

Figure S17. Emission spectra of an emulsion of **1** in 5ml toluene in the presence of different concentrations of methanol (excited at 380 nm).

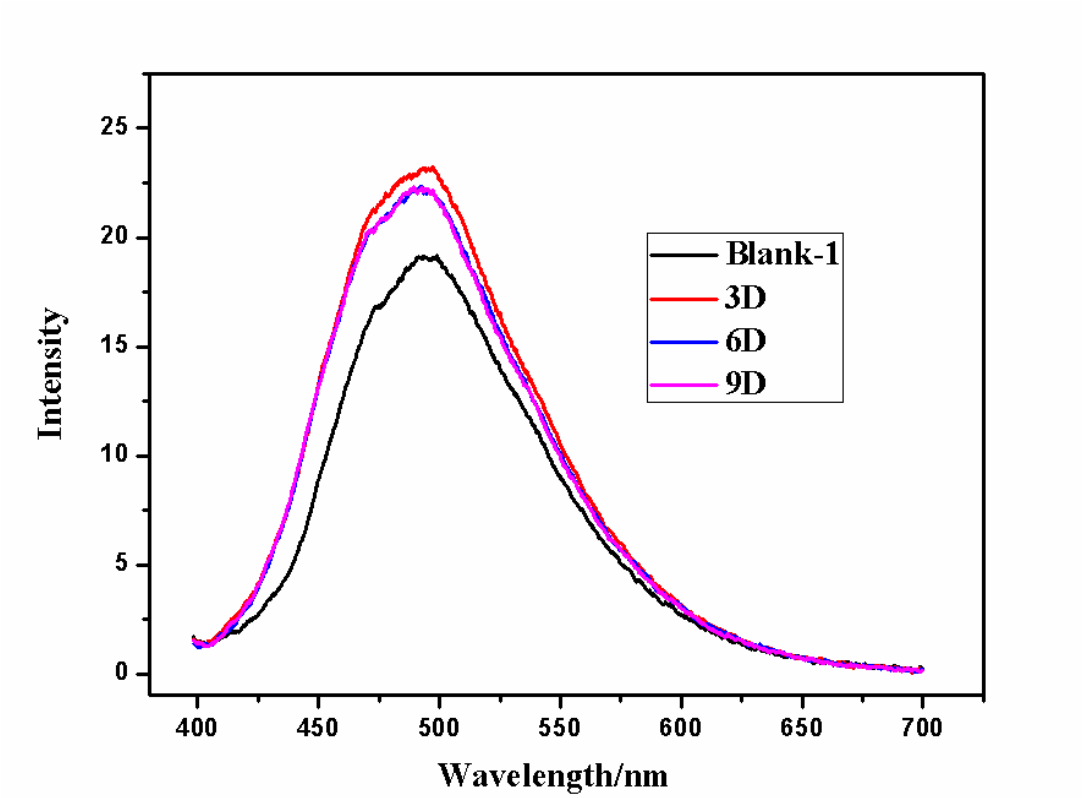

Figure S18. Emission spectra of an emulsion of **1** in 5ml toluene in the presence of different concentrations of ethanol (excited at 380 nm).

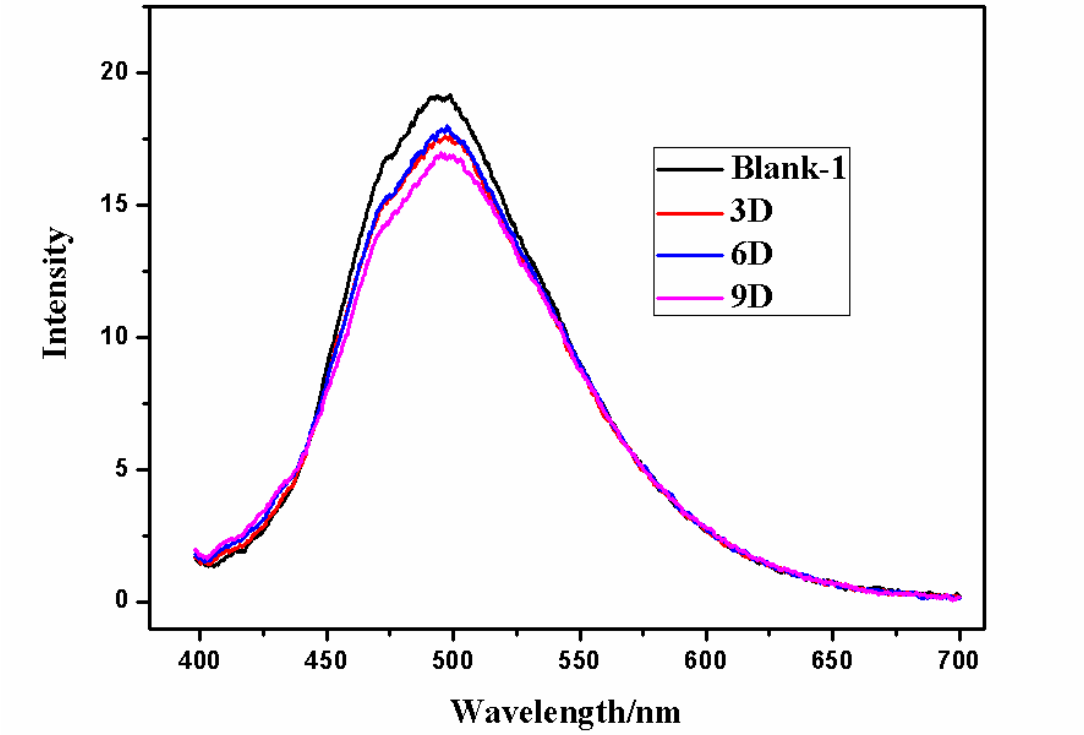

Figure S19. Emission spectra of an emulsion of **1** in 5ml toluene in the presence of different concentrations of acetonitrile (excited at 380 nm).

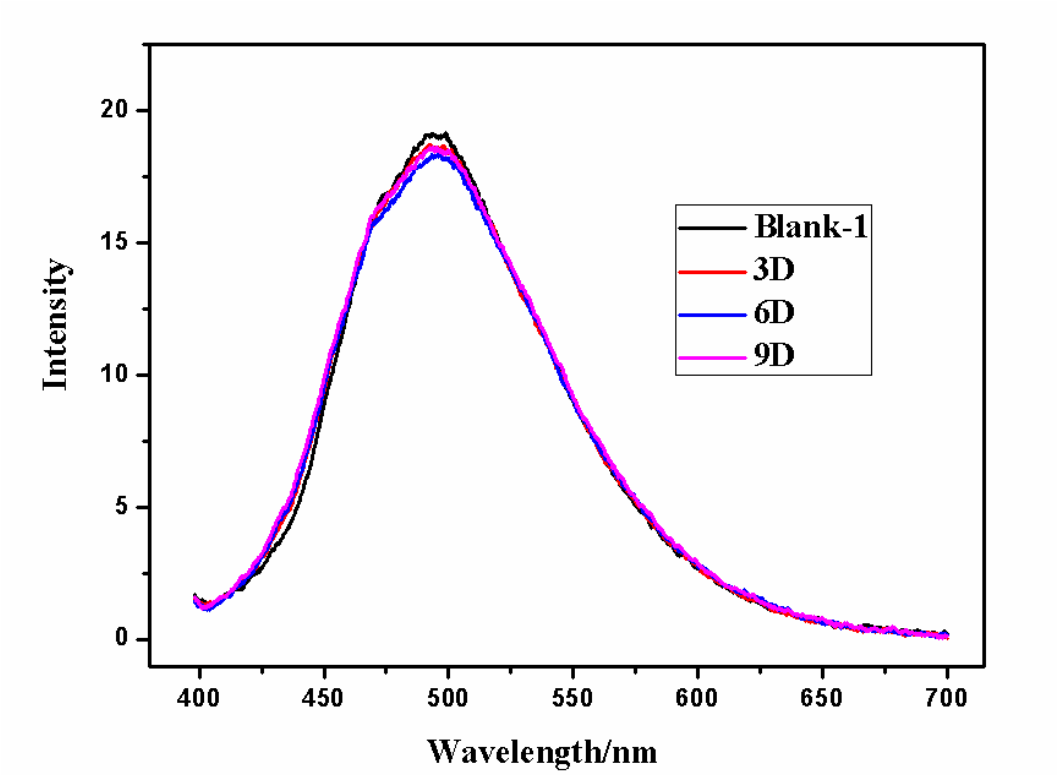

Figure S20. Emission spectra of an emulsion of **1** in 5ml toluene in the presence of different concentrations of 2-propanol (excited at 380 nm).

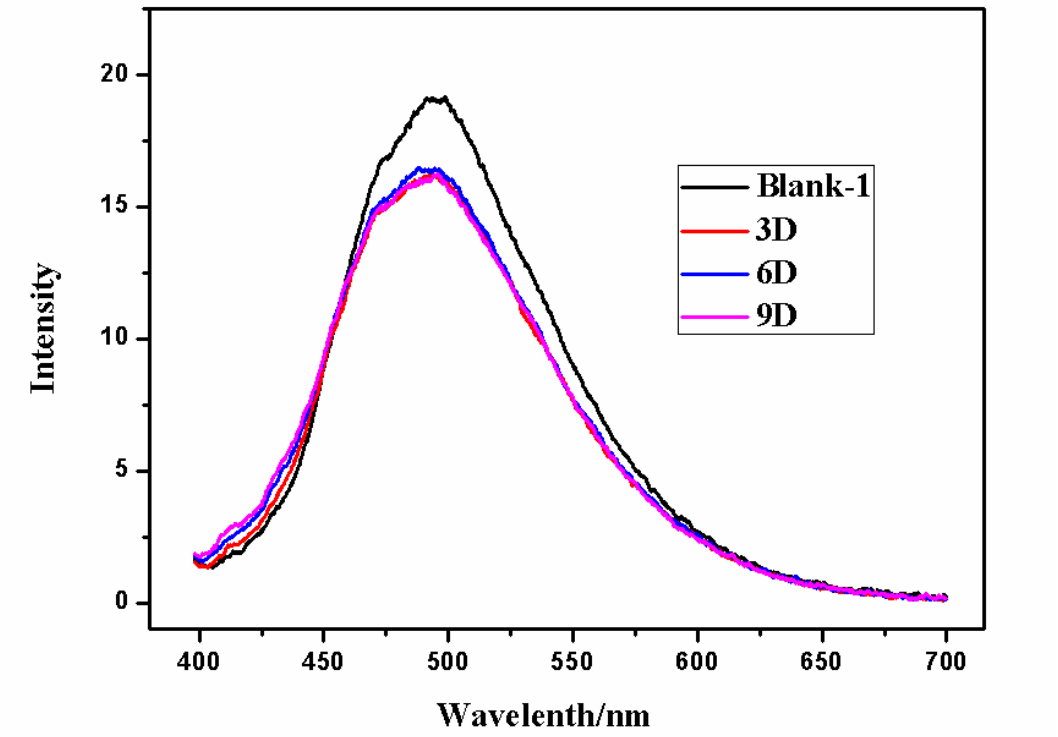

Figure S21. Emission spectra of an emulsion of **1** in 5ml toluene in the presence of different concentrations of 1-propanol (excited at 380 nm).

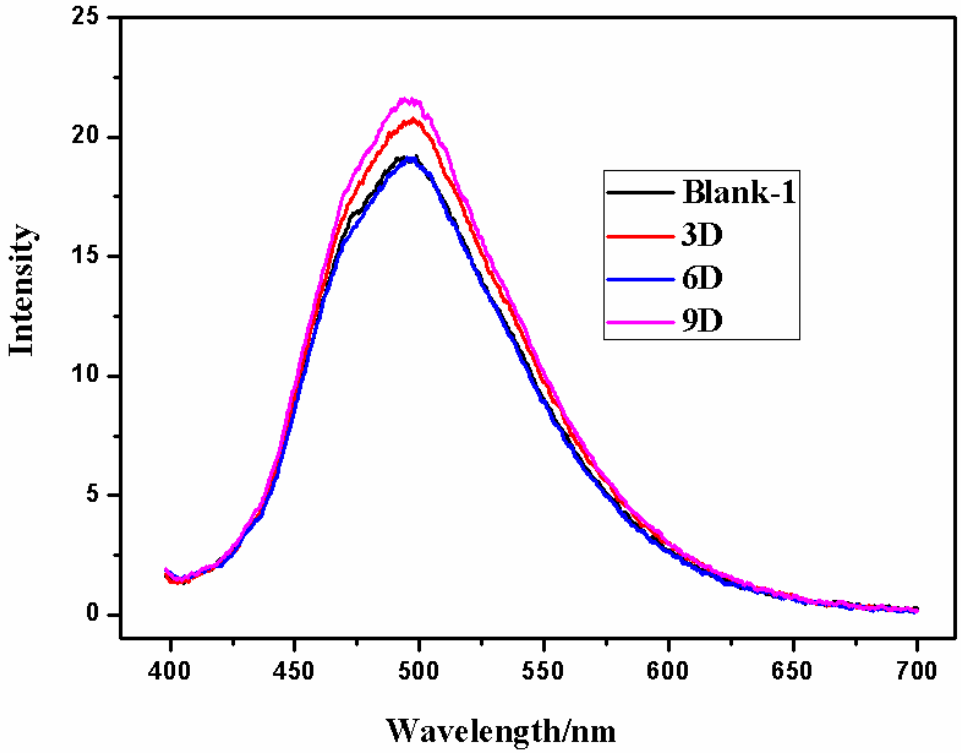

Figure S22. Emission spectra of an emulsion of **1** in 5ml toluene in the presence of different concentrations of hexane (excited at 380 nm).

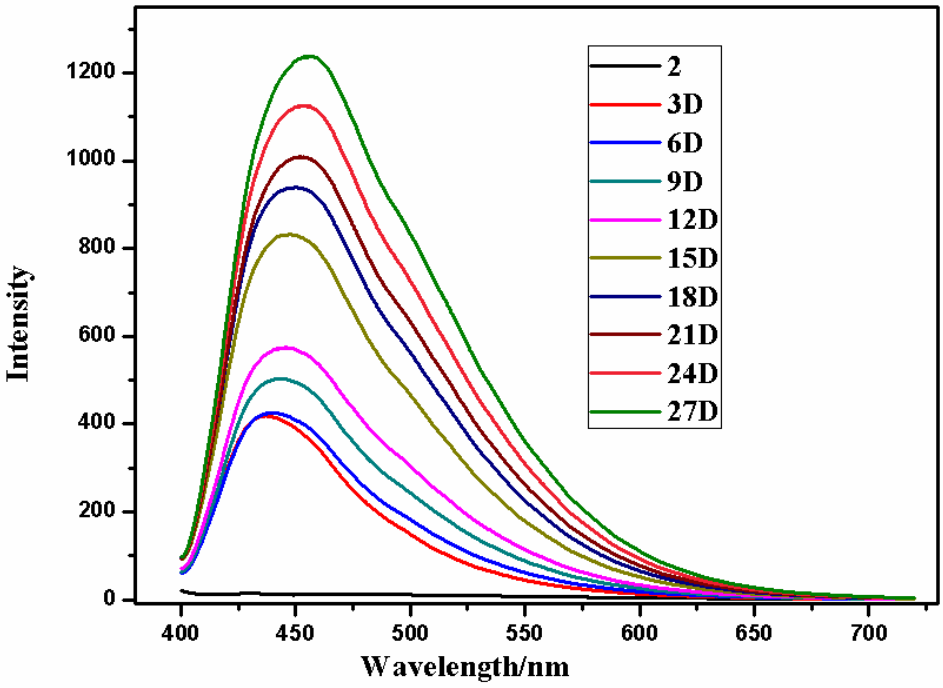

Figure S23. Emission spectra of an emulsion of **2** in 5ml toluene in the presence of different concentrations of DMSO (excited at 380 nm).

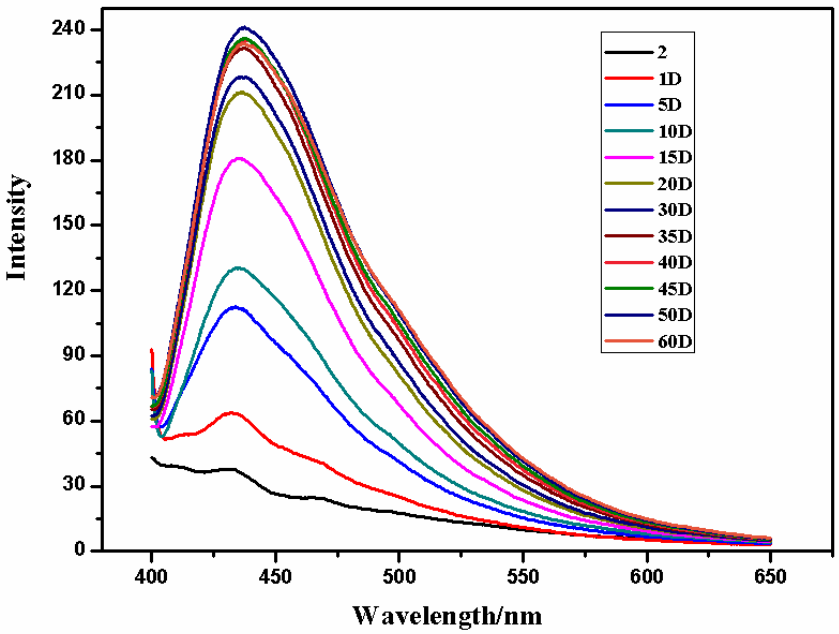

Figure S24. Emission spectra of an emulsion of **2** in 5ml toluene in the presence of different concentrations of DMF (excited at 380 nm).

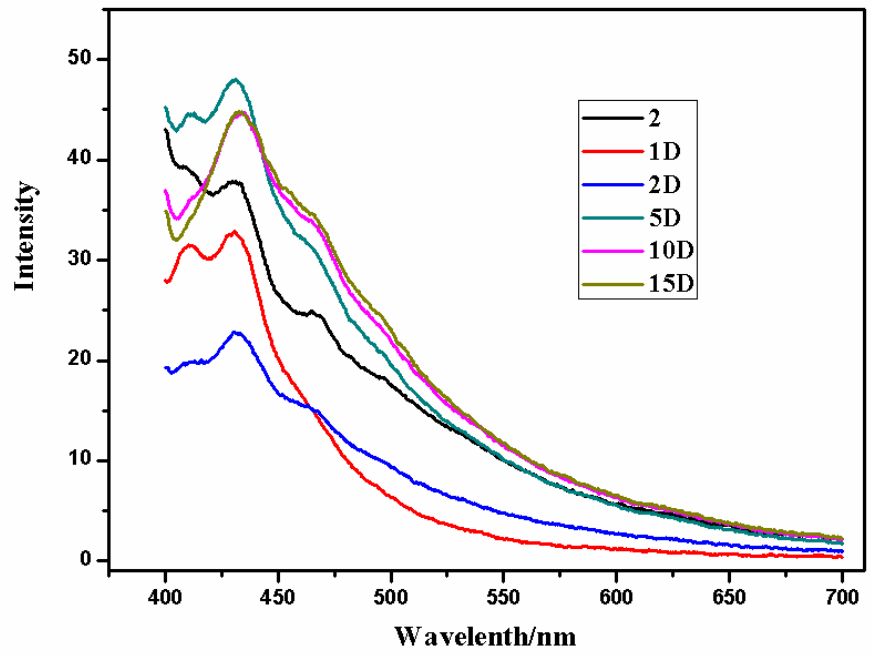

Figure S25. Emission spectra of an emulsion of **2** in 5ml toluene in the presence of different concentrations of THF (excited at 380 nm).

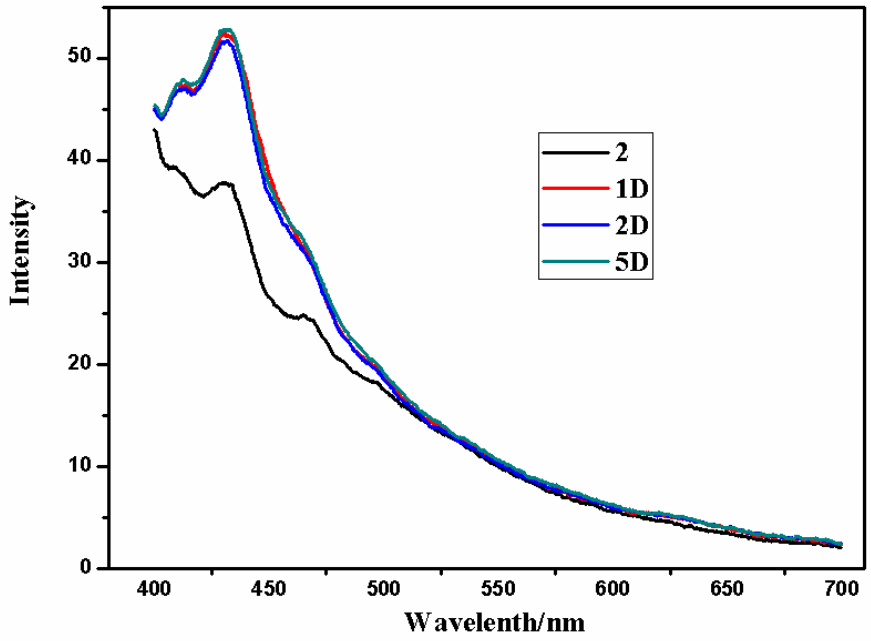

Figure S26. Emission spectra of an emulsion of **2** in 5ml toluene in the presence of different concentrations of acetone (excited at 380 nm).

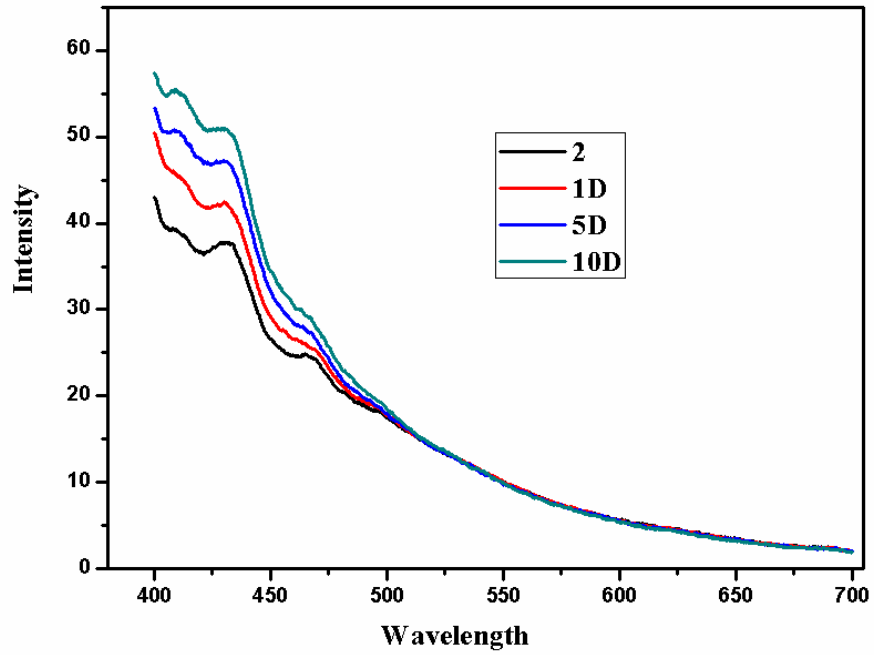

Figure S27. Emission spectra of an emulsion of **2** in 5ml toluene in the presence of different concentrations of dichloromethane (excited at 380 nm).

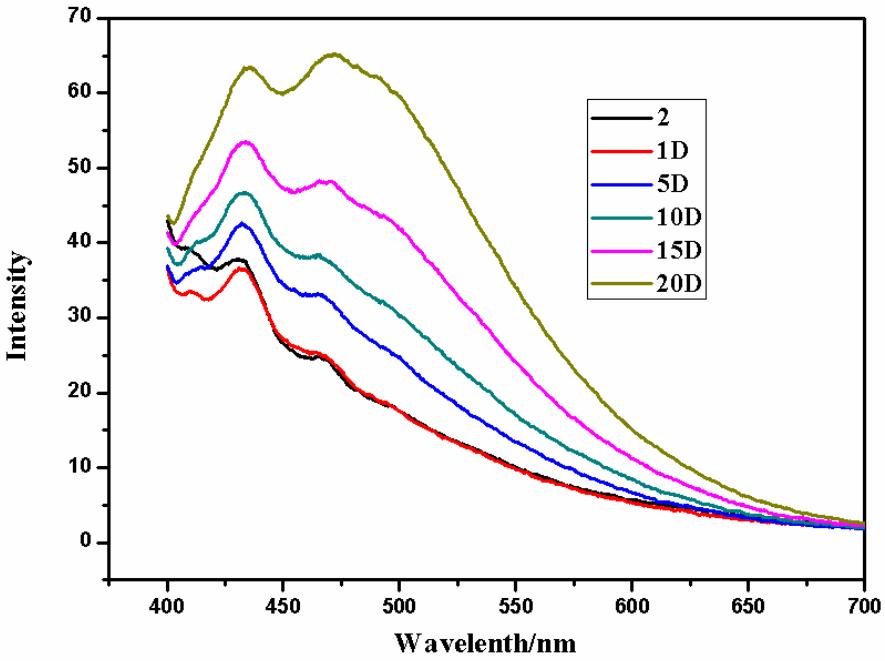

Figure S28. Emission spectra of an emulsion of **2** in 5ml toluene in the presence of different concentrations of methanol (excited at 380 nm).

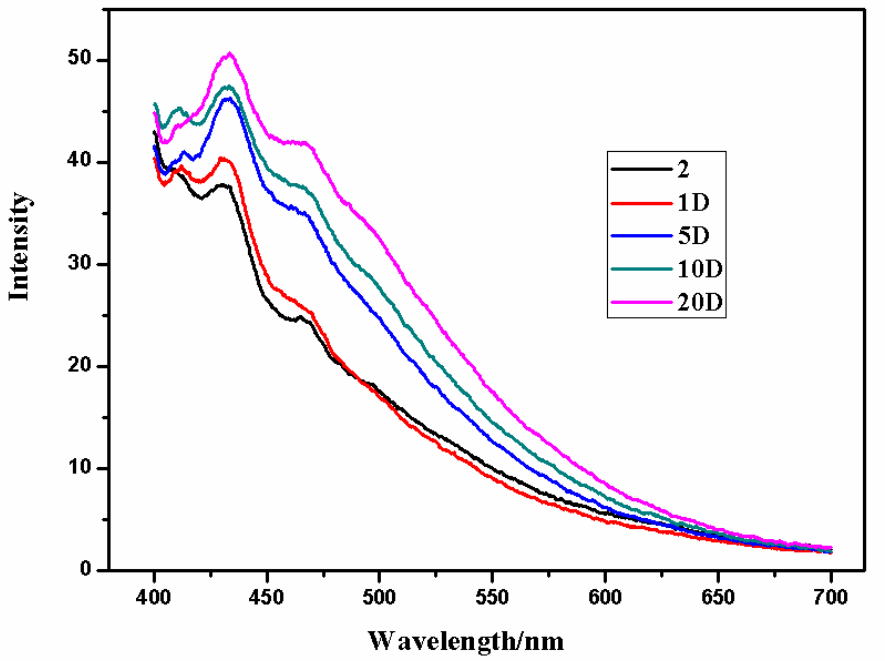

Figure S29. Emission spectra of an emulsion of **2** in 5ml toluene in the presence of different concentrations of ethanol (excited at 380 nm).

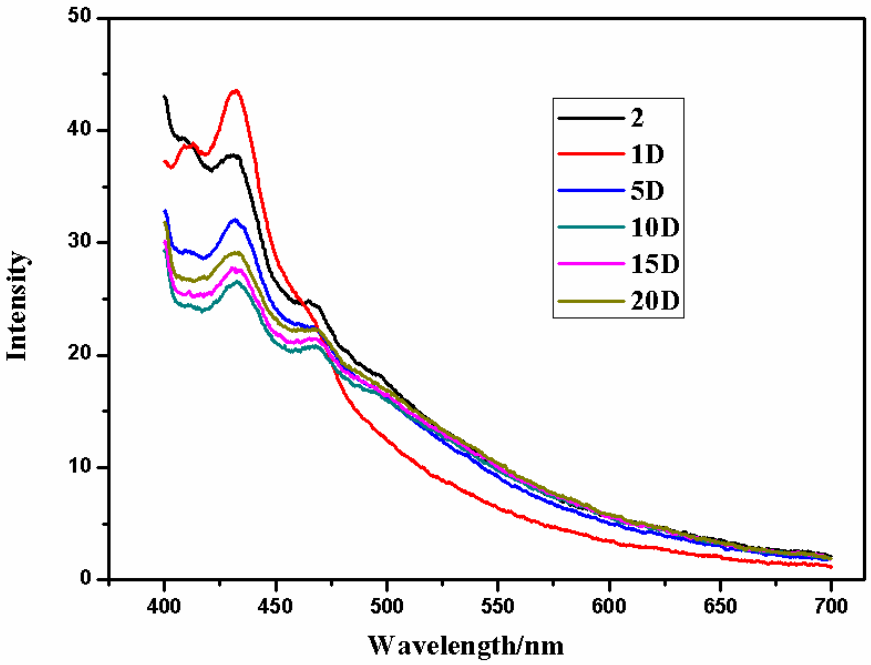

Figure S30. Emission spectra of an emulsion of **2** in 5ml toluene in the presence of different concentrations of acetonitrile (excited at 380 nm).

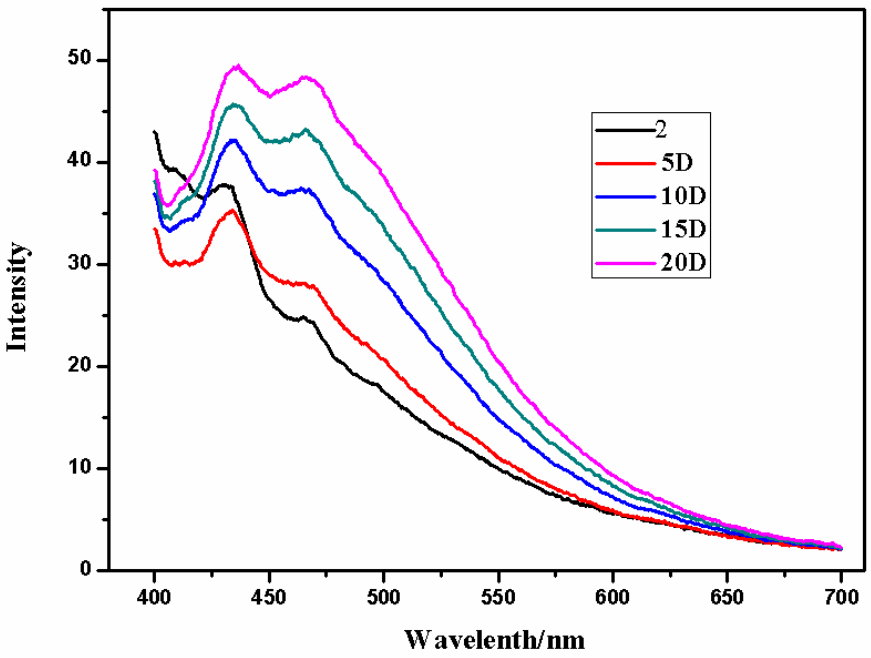

Figure S31. Emission spectra of an emulsion of **2** in 5ml toluene in the presence of different concentrations of 2-propanol (excited at 380 nm).

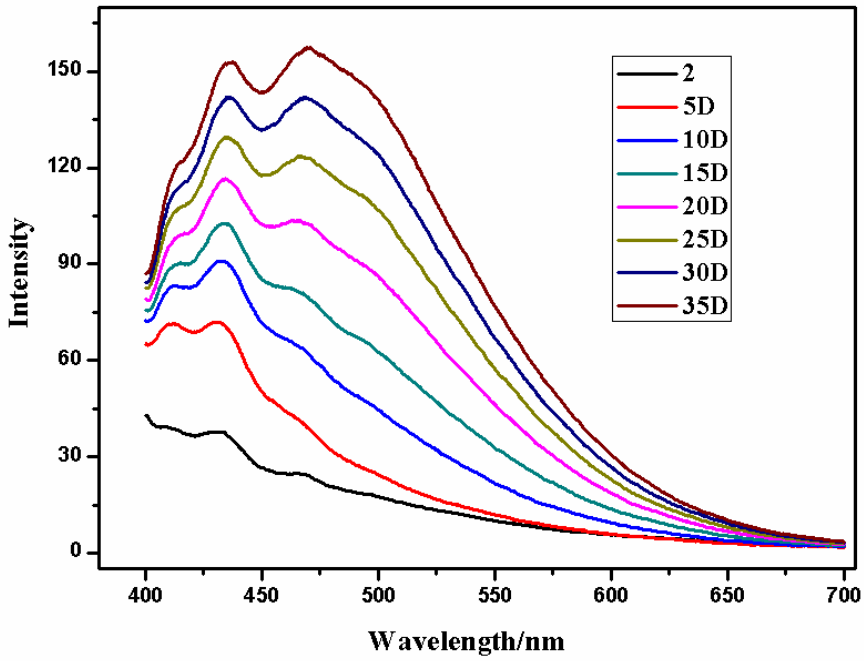

Figure S32. Emission spectra of an emulsion of **2** in 5ml toluene in the presence of different concentrations of 1-propanol (excited at 380 nm).

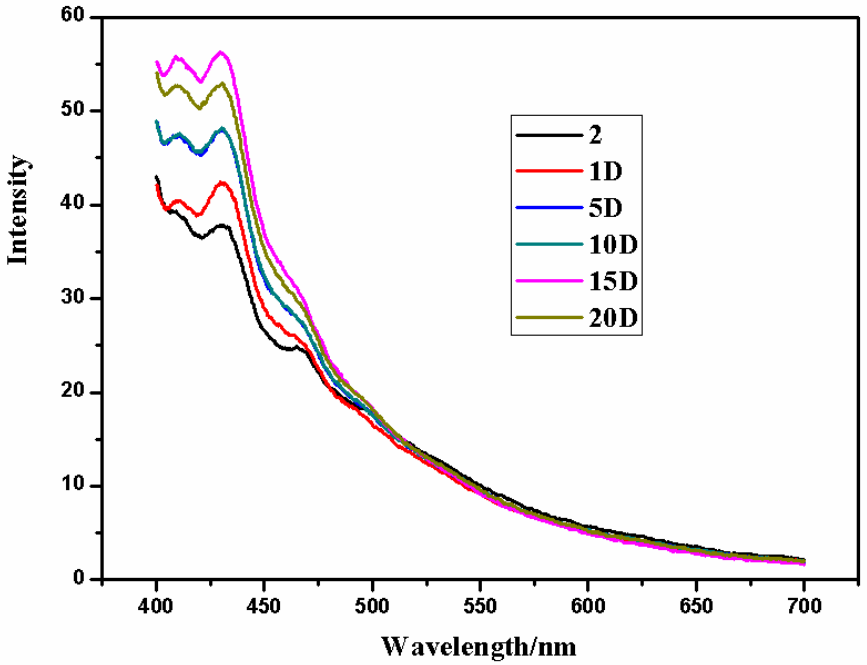

Figure S33. Emission spectra of an emulsion of **2** in 5ml toluene in the presence of different concentrations of hexane (excited at 380 nm).

(10) The sensing of metal ions of 2

The as-synthesized sample of **2** (4.0 mg) was ground and suspended in DMF solution (5 ml), to which was added different metal ions.

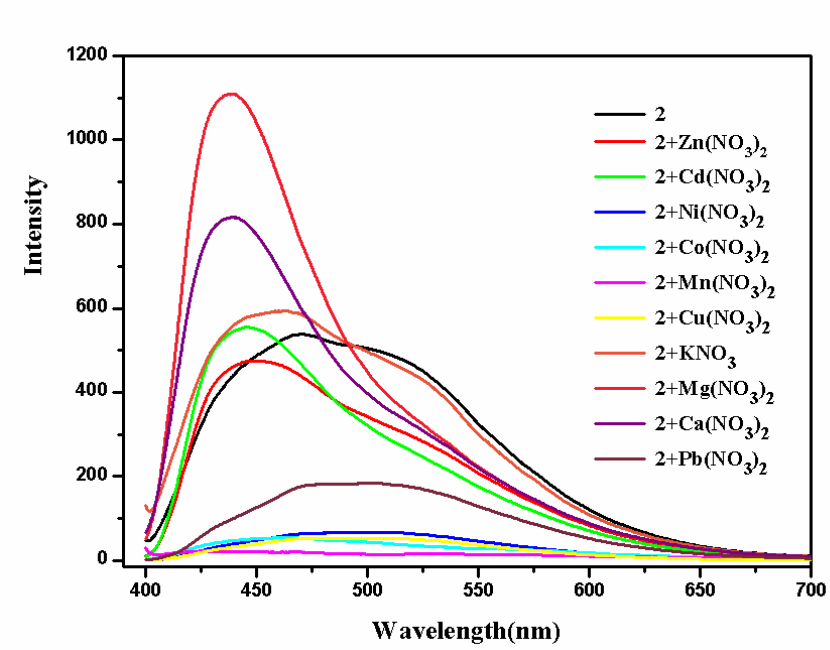

Figure S34. Emission spectra of an emulsion of **2** in 5ml DMF in the presence of different metal ions (excited at 380 nm).

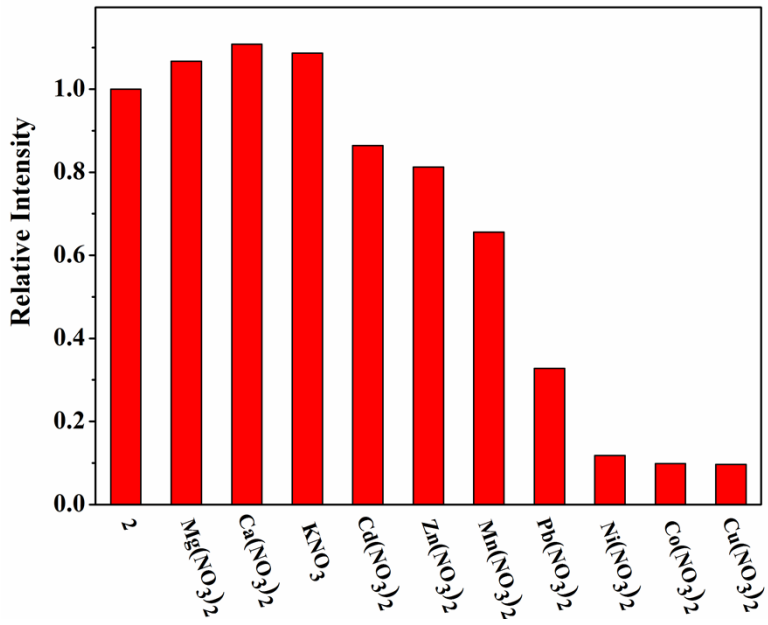

Figure35. Photoluminescence intensity of **2** treated with different metal ions (10^{-2} M) in DMF solution.

References

1. F. Gándara, B. Gómez-Lor, M. Iglesias, N. Snejko, E. Gutiérrez-Puebla, A. Monge, *Chem. Commun.,* 2009, 2393-2395.

2. P. Phuengphai, S. Youngme, P. Gamez, J. Reedijk, *Dalton Trans.,* 2010, **39**, 7936-7942.

3. A. Henschel, K. Gedrich, R. Kraehnert, S. Kaskel, *Chem. Commun.,* 2008, 4192-4194.

4. H. F. Yao, Y. Yang, H. Liu, F. G. Xi, E. Q. Gao, *Journal of Molecular Catalysis A: Chemical.,* 2014, **394**, 57-65.

5. D. B. Dang, P. Y. Wu, C. He, Z. Xie, Y. C. Duan, *J. Am. Chem. Soc.,* 2010, **132**, 14321-14323.

6. D'Vries, R. F.; de la Pena-O'Shea, V. A.; Snejko, N.; Iglesias, M.; Gutiérrez-Puebla, E.; Monge, M. A. *Cryst. Growth Des.,* 2012, **12**, 5535-5545.

7. S. Nayak, K. Harms, S. Dehnen, *Inorg. Chem.,* 2011, **50**, 2714-2716.

8. Q. X. Han, X. P. Sun, J. Li, P. T. Ma, J. Y. Niu, *Inorg. Chem.,* 2014, **53**, 6107-6112.

9. T. Kajiwara, M. Higuchi, A. Yuasa, *Chem. Commun*., 2013, **49**, 10459-10461.

10. S. Horike, M. Dincă, K. Tamaki, J. R. Long, *J. Am. Chem. Soc.,* 2008, **130**, 5854-5855.

11. Y. Zhu, Y. M. Wang, J. Xu, P. Liu, H.A.B.M.D. Weththainha, Y. L. Wu, X. Q. Lu, J. M. Xie, *Journal of Solid State Chemistry* , 2014, **219**, 259-264.

12. K. K. Raja. D. Easwaramoorthy, K. Rani, J. Rajesh, Y. Jorapurd, S. Thambidurai, P. R. Athappanc, G. Rajagopala, *Journal of Molecular Catalysis A: Chemical,* 2009, **303**, 52-59.

13. Y. Zhu, Y. M. Wang, S. Y. Zhao, P. Liu, C. Wei, Y. L. Wu, C. K. Xia, J. M. Xie, *Inorg. Chem.,* 2014, **53**, 7692-7699.

14. X. M. Lin, T. T. Li, Y. W. Wang, L. Zhang, C. Y. Su, *Chem. Asian J.,* 2012, **7**, 2796-2804.

15. R. Fernández de Luis, M. K. Urtiaga, J. L. Mesa, E. S. Larrea, M. Iglesias, T. Rojo, M. I. Arriortua, *Inorg. Chem.,* 2013, **52**, 2615-2626.

16. M. Gustafsson, A. Bartoszewicz, B. Martín-Matute, J. L. Sun, J. Grins, T. Zhao, Z. Y. Li, G. S. Zhu, X. D. Zou, *Chem. Mater.,* 2010, **22**, 3316-3322.

17. R. F. D'Vries, V. A. de la Pena-O'Shea, N. Snejko, M. Iglesias, E. Gutiérrez-Puebla, M. A. Monge, *J. Am. Chem. Soc*., 2013, **135**, 5782-5792.

18. R. F. D'Vries, M. Iglesias, N. Snejko, E. Gutiérrez-Puebla, M. A. Monge, *Inorg. Chem.,* 2012, **51**, 11349-11355.

19. K. Mo, Y. H. Yang, Y. Cui, *J. Am. Chem. Soc.,* 2014, **136**, 1746-1749.

20. A. C. Kathalikkattil, D. W. Kim, J. Tharun, H. G. Soek, R. Roshan, D. W. Park, *Green Chem.,* 2014, **16**, 1607-1616.

21. J. L. Song, Z. F. Zhang, S. Q. Hu, T. B. Wu, T. Jiang, B. X. Han, *Green Chem.,* 2009, **11**, 1031-1036.

22. W. Y. Gao, Y. Chen, Y. Niu, K. Williams, L. Cash, P. J. Perez, L. Wojtas, J. F. Cai, Y. S. Chen, S. Q. Ma, *Angew. Chem. Int. Ed.,* 2014, **53**, 2615-2619.

23. V. Guillerm, Ł. J. Weseliński, Y. Belmabkhout, A. J. Cairns, V. D′Elia, Ł. Wojtas, K. Adil, M. Eddaoudi, *Nat. Chem*., 2014, **6**, 673-680.

24. Y. W. Ren, Y. C. Shi, J. X. Chen, S. R. Yang, C. R. Qi, H. F. Jiang, *RSC Adv.,* 2013, **3**, 2167-2170.

25. T. Lescouet, C. Chizallet, D. Farrusseng, *ChemCatChem.,* 2012, **4**, 1725-1728.

26. X. Q. Huang, Y. F. Chen, Z. G. Lin, X. Q. Ren, Y. N. Song, Z. Z. Xu, X. M. Dong, X. G. Li, C. W. Hu, B. Wang, *Chem. Commun*., 2014. **50**, 2624-2627.

27. B. Delley, *J. Chem. Phys.,* 1990, **92**, 508-517.

28. B. Delley, *J. Chem. Phys.,* 1996, **100**, 6107-6110.

29. B. Delley, *J. Chem. Phys.,*2000, **113**, 7756-7764.

30. J. P. Perdew, Y. Wang, *Phys. Rev. B,* 1992, **45**, 13244-13249.

31. J. P. Perdew, Y. Wang, *Phys. Rev. B,* 1986, **33**, 8800-8802.

32. B. Delley, *Phys. Rev. B,* 2002, **66**, 155125.

33. C. Chizallet, S. Lazare, D. Bazer-Bachi, F. Bonnier, V. Lecocq, E. Soyer, A-A. Quoineaud, N. Bats, *J Am Chem Soc.,* 2010, **132**, 12365-12377.

34. P. Ryan, I. Konstantinov, R. Q. Snurr, L. J. Broadbelt, *J. Catal.,* 2012, **286**, 95-102.

35. D. Liu, C. L. Zhong, *J Phys Chem Lett.,* 2009, **1**, 97.

36. F. Vermoortele, M. Vandichel, B. V. de Voorde, R. Ameloot, M. Waroquier, V. V. Speybroeck, D. E. De Vos, *Angew. Chem. Int. Ed.,* 2012, **51**, 4887-4890.

37. A. E. Reed, L. A. Curtiss, F. Weinhold, *Chem. Rev.,* 1988, **88**, 899-926.

38. A. D. Becke, *J. Chem. Phys.,*1993, **98**, 5648-5652.

39. C. Lee, W. Yang, R. G. Parr, *Phys. Rev. B,* 1988, **37**, 785-789.

40. Krishnan, J. S. Binkley, R. Seeger, J. A. Pople, *J. Chem. Phys*., 1980, **72**, 650-654.

41. J. P. Blaudeau, M. P. McGrath, L. A. Curtiss, L. Radom, *J. Chem. Phys*., 1997, **107**, 5016-5023.

42. T. Clark, J. Chandrasekhar, P. V. R. Schleyer, *J. Chem. Phys.,*1983, **74**, 294.

43. M. J. Frisch, G. W. Trucks, H. B. Schlegel, G. E. Scuseria, M. A. Robb, J. R. Cheeseman, J. A. Jr. Montgomery, T. Vreven, K. N. Kudin, J. C. Burant, J. M. Millam, S. S. Iyengar, J. Tomasi, V. Barone,

B. Mennucci, M. Cossi, G. Scalmani, N. Rega, G. A. Petersson, H. Nakatsuji, M. Hada, M. Ehara, K. Toyota, R. Fukuda, J. Hasegawa, M. Ishida, T. Nakajima, Y. Honda, O. Kitao, H. Nakai, M. Klene, X. Li, J. E. Knox, H. P. Hratchian, J. B. Cross, C. Adamo, J. Jaramillo, R. Gomperts, R. E. Stratmann, O. Yazyev, A. J. Austin, R. Cammi, C. Pomelli, J. W. Ochterski, P. Y. Ayala, K. Morokuma, G. A. Voth, P. Salvador, J. J. Dannenberg, V. G. Zakrzewski, S. Dapprich, A. D. Daniels, M. C. Strain, O. Farkas, D. K. Malick, A. D. Rabuck, K. Raghavachari, J. B. Foresman, J. V. Ortiz, Q. Cui, A. G. Baboul, S. Clifford, J. Cioslowski, B. B. Stefanov, G. Liu, A. Liashenko, P. Piskorz, I. Komaromi, R. L. Martin, D. J. Fox, T. Keith, M. A. Al-Laham, C. Y. Peng, A. Nanayakkara, M. Challacombe, Gill, B. Johnson, W. Chen, M. W. Wong, C. Gonzalez, J. A. Pople, Gaussian 03, revision B.05; Gaussian, Inc.: Pittsburgh, PA, 2003.